 Bull. Chem. Soc. Jpn. Vol. 84, No. 7, 679–697 (2011)

Award Accounts

The Chemical Society of Japan Award for 2009

Subporphyrins: A Legitimate Ring-Contracted Porphyrin with Versatile Electronic and Optical Properties

Atsuhiro Osuka,* Eiji Tsurumaki, and Takayuki Tanaka

Department of Chemistry, Graduate School of Science, Kyoto University, Sakyo-ku, Kyoto 606-8502

Received April 25, 2011; E-mail: osuka@kuchem.kyoto-u.ac.jp

After a brief survey of our efforts in the development of novel porphyrinoids that include *meso–meso*-linked porphyrin arrays, *meso*-aryl expanded porphyrins, and transition-metal-catalyzed functionalizations of porphyrins, a particular focus in this account is placed on the chemistry of subporphyrins that has been explored in our group. Subporphyrin is a legitimate ring-contracted porphyrin consisting of three pyrrolic subunits domed in a C_3 symmetric bowl shape. While subporphyrins are simple and small macrocycles and possess a key position in porphyrin chemistry, they had been elusive until our first synthesis of tribenzosubporphines in 2006. Shortly after, synthetic protocols of *meso*-aryl-substituted subporphyrins were developed to produce various subporphyrins with versatile electronic properties that can be widely tuned by *meso*-aryl substituents. Raney nickel reduction was used to prepare *meso*-alkyl-substituted subporphyrins from *meso*-thienyl-substituted subporphyrins. Subchlorins and subbacteriochlorins were prepared respectively by the reduction of subporphyrins with *p*-tosylhydrazide and Raney nickel. While subporphyrins and subchlorins share conjugated 14π-electronic circuits, subbacteriochlorins have a rare [13]diazaannulene circuit maintained through the lone-pair electrons of the nitrogen atom. The aromaticity decreases in the order of subporphyrin > subchlorin > subbacteriochlorin, as indicated from ^{1}H- and ^{11}B NMR spectra and nuclear independent chemical shift (NICS) calculations. Despite these progresses, the chemistry of subporphyrins is still in the infant stage with many untouched aspects and further improvements in synthetic yields are highly desirable for the developments of the chemistry of subporphyrins as well as their applications in diverse fields.

1. A Brief Survey of Our Efforts in the Exploration of Novel Porphyrinoids

In the last three decades, we have been involved in the exploration of novel porphyrinoids with intriguing structures, electronic and optical properties, and functions. We entered porphyrin chemistry with the aim to synthesize covalently linked organic constructs that can mimic the whole excitation energy transfer and electron transfer events of the photosynthetic reaction centers within a single molecular entity.[1–3] In the course of these studies, we fortunately encountered new reactions and structures, which drove us to change our research style from a well-designed, goal-orientated path to a flexible discovery-searching strategy to explore novel porphyrinoids. By following the flexible research style, we have explored *meso–meso*-linked Zn(II) porphyrin arrays, *meso*-aryl expanded porphyrins, transition-metal-catalyzed porphyrin modifications, and subporphyrins. After a brief survey of the former three topics, a particular focus is placed on the chemistry of subporphyrins that are legitimate ring-contracted porphyrins. As described below, subporphyrins are a new class of functional molecules, particularly in view of their highly tunable electronic and optical properties.

1.1 *meso–meso*-Linked Porphyrin Arrays. In 1997 we reported Ag(I)-promoted *meso–meso* coupling reaction of 5,15-diaryl Zn(II) porphyrins.[4] This reaction was accidentally found during the preparation of a *meso*-nitrated Zn(II) porphyrin by nitration of 5,15-diaryl Zn(II) porphyrin with $AgNO_2$ and I_2 by following Baldwin and Crossley's protocol.[5] The standard coupling protocol is a very simple treatment of 5,15-diaryl Zn(II) porphyrin with $AgPF_6$ in $CHCl_3$ at room temperature. It is important to monitor the progress of the reaction, for instance by gel-permeation chromatography (GPC) HPLC or ^{1}H NMR spectroscopy, to quench the reaction at a conversion of 30–40%, since further reaction leads to the production of larger porphyrin arrays, which makes the separation of the products more difficult. Usually the coupling products are separated from a starting substrate by GPC-HPLC. This coupling reaction has proven very effective, particularly for large porphyrin substrates.[6] It is amazing that extremely long porphyrin arrays (even 128-mer and 256-mer) smoothly undergo the coupling reaction, although they bear only two edge free *meso*-positions that can be used for the coupling. On the basis of this coupling reaction, we prepared extremely long porphyrin arrays up to linear 1024-mer,[6] three-dimensionally extending windmill porphyrin arrays,[7–9] dihedral angle controlled *meso–meso*-

Published on the web July 2, 2011; doi:10.1246/bcsj.20110118

linked diporphyrins,[10,11] large porphyrin wheels,[12–14] helical porphyrin arrays held by intermolecular hydrogen bonding host–guest interaction,[15] and directly linked porphyrin rings.[16] *meso–meso*-Linked diporphyrin motifs are suitable for supramolecular assembling. Along this strategy three-dimensional porphyrin boxes and other interesting architectures have been constructed through rigorous self-sorting assembly of pyridine-appended or cinchomeronimide-appended *meso–meso*-linked Zn(II) diporphyrins.[17–20] In the meanwhile, we explored an effective oxidative ring-closure reaction initially with tris(4-bromophenyl)aminium hexachloroantimonate[21,22] and later with the combined use of 2,3-dichloro-5,6-dicyano-1,4-benzoquinone (DDQ) and $Sc(OTf)_3$.[23] The latter method is superior to the former because of the absence of serious halogenation side products, and allows the conversion of long *meso–meso*-linked Zn(II) porphyrin arrays to corresponding *meso–meso*, β–β, β–β triply linked porphyrin arrays that are called porphyrin tapes.[23] On the basis of this oxidation, we have explored extensively π-conjugated porphyrin tapes that display remarkably red-shifted and enhanced absorptions reaching deep in the infrared region,[23–26] an antiaromatic tetrameric porphyrin sheet that exhibits a strong paratropic ring current above the central planar cyclooctatetraene core,[27] and two-dimensionally extending porphyrin tapes.[28] The bay-area selective cycloaddition reactions of porphyrin tapes proceeded nicely with an *o*-xylylene[29a] and an azomethine ylide.[29b] Interesting porphyrin tape variants have been also explored by Diederich et al.,[30–32] Aida et al.,[33–35] and Anderson et al.[36] The chemistry of *meso–meso*-linked porphyrin arrays and porphyrin tapes have been reviewed elsewhere.[37–45]

1.2 *meso*-Aryl Expanded Porphyrins. In the last three decades, the chemistry of expanded porphyrins has been actively explored in light of their favorable attributes such as rich coordination chemistry, anion sensing, large two-photon absorption cross-sections, and extended π-electronic systems.[46–55] The *meso*-aryl expanded porphyrins can be regarded as legitimate expanded porphyrins in terms of the regular and alternate arrangements of pyrroles and aryl-substituted methine carbons. Except [26]- and [28]hexaphyrins(1.1.1.1.1.1),[56] almost nothing had been known about these macrocycles until our first report. We serendipitously found the formation of a series of *meso*-aryl expanded porphyrins during the synthesis of tetrakis(pentafluorophenyl)porphyrin by the Lindsey method[57] using pentafluorobenzaldehyde and pyrrole. We made a fortunate mistake in running the reaction at substrate concentrations of 67 mM, ca. 10-fold higher than the optimized concentration for porphyrin synthesis.[58,59] Under these conditions, a series of *meso*-aryl expanded porphyrins including *N*-fused pentaphyrins, hexaphyrin, heptaphyrin, octaphyrin, nonaphyrin, decaphyrin, undecaphyrin, and dodecaphyrin were formed effectively in a surprising manner,[59] which were very difficult to separate. Separation difficulty has been somewhat mitigated by size-selective synthesis of the expanded porphyrins using a dipyrromethane and a tripyrromethane as precursors.[60,61] Use of high concentrations of the substrates led to better yields of larger expanded porphyrins.[62] These *meso*-aryl expanded porphyrins have proven to be attractive platforms for rich coordination chemistry,[63–69] versatile aromatic compounds such as strongly Hückel aromatic[64,65,70] and antiaromatic,[64,65] Möbius aromatic[71–80] and antiaromatic[81,82] species, stable organic radical species,[70,83,84] and unprecedented rearrangements triggered by transannular electronic interactions.[85,86] Beside these, the *meso*-aryl expanded porphyrins are quite interesting from the viewpoint of mutual chemical interconversions (metamorphosis).[87,88] The most remarkable example is the efficient and quantitative splitting reaction of bis-Cu(II) complex of a [36]octaphyrin into two molecules of Cu(II) porphyrins upon heating.[89] This transformation requires the rapture and formation of two carbon–carbon double bonds in a metathesis manner.[90] It has been thought that the transannular electronic interaction is enhanced at the hinge position of a figure-eight conformation of the octaphyrin upon the metalation. We have also demonstrated that the similar metathesis-like splitting reactions of B(III)–Cu(II) hybrid complexes of [32]heptaphyrins to B(III) [14]subporphyrin and Cu(II) [18]porphyrin,[91,92] the B(III) metalation-induced skeletal rearrangement from [28]hexaphyrin(1.1.1.1.1.1) to B(III) coordinated [28]hexaphyrin(2.1.1.0.1.1) via a transposition of a pentafluorophenyl-substituted *meso*-methine carbon,[93] Pd(II) metalation-induced formation of an *N*-confused porphyrin segment from [32]heptaphyrin substrates,[94] and Ni(II) metalation induced formation of a directly *meso*–β-linked diporphyrin.[95] The chemistry of expanded porphyrins have been reviewed elsewhere,[52–55,96] where the emphasis was placed on the chemical reactivity and aromaticity.

1.3 Iridium-Catalyzed β-Selective C–H Activated Direct Borylation. Peripheral modifications of porphyrins are effective for the tuning of the electronic properties, the exploration of functional porphyrins, and the covalent linking of porphyrins.[97–103] Recently, transition-metal-catalyzed reactions have been often used for this purpose. Representative examples are Sonogashira coupling,[104–106] Stille coupling,[107] Suzuki–Miyaura coupling,[108,109] and Co(II)-catalyzed alkyne trimerization reactions.[110–114] In 2005, we found that iridium-catalyzed C–H activated direct borylation reaction of 5,15-diaryl porphyrins proceeded nicely with high yield and perfect regioselectivity at β-positions next to free *meso*-positions.[115] Following the synthetic protocol developed by Miyaura and Ishiyama,[116,117] we have synthesized a variety of β-borylated porphyrins and β,β-diborylated porphyrins, which are nice precursors of functional porphyrins and covalently linked porphyrin oligomers. Representative examples synthesized through this method include β,β-bis(acrylyl)-substituted porphyrins that can serve as an effective sensitizer in solar cells,[118,119] multi-porphyrin oligomers,[120,121] planar doubly 1,3-butadiyne-bridged diporphyrins,[122] heterocycle-bridged porphyrin rings,[123–125] 2-borylated corroles,[126] biscorrole-based stable singlet biradicals,[127,128] face-to-face dioxoisobacteriochlorin dimers,[129] porphyrin pincer complexes that exhibited catalytic activity in Heck reactions,[130] Pt–pincer complexes that undergo tweezers-like molecular motions responding to the oxidation state of the incorporated Pt metal,[131] and η^2 coordinating Ru(II) complexes.[132] Recent remarkable examples are β,β-doubly linked porphyrin belts with significant molecular curvatures[133] and ring forming porphyrin barrels,[134] both of which can capture C_{60} efficiently. These results are reviewed elsewhere with exceptions of recent examples.[135]

2. Subporphyrins

2.1 Introduction. Subporphyrin, a porphyrinic counterpart of subphthalocyanine **1** (Figure 1), is a genuine ring-contracted porphyrin that possesses a regular arrangement of three pyrrole units bridged by methine carbon atoms to constitute a conjugated 14π-aromatic circuit.[136] Subporphyrin is a recent newcomer in the porphyrinoid family, and it had been elusive until the first synthesis of tribenzosubporphine **2** by our group in 2006.[137] This situation sharply contrasts with subphthalocyanine **1**, which was first synthesized by Meller and Ossko in 1972.[138] The chemistry of subphthalocyanine **1** and related compounds such as subporphyrazine **3** has been actively developed in light of bowl-shaped triangular π-conjugation, intense visible absorption and fluorescence, nanoscale science, and nonlinear optical properties.[139–141] This marked difference between subporphyrin and subphthalocyanine is due mainly to different synthetic availability. Subphthalocyanines can be prepared in good yields from a variety of phthalonitrile derivatives via cyclotrimerization with aid of boron template, whereas no synthetic method had existed for subporphyrins until our report despite their relatively simple structures.

2.2 Tribenzosubporphines. Tribenzosubporphine was synthesized under harsh conditions, using Gouterman's protocol with some modifications (Scheme 1).[142] Heating of a well-ground solid mixture of boric acid and 2-(3-oxo-2,3-dihydro-1*H*-isoindol-1-yl)acetic acid at 350 °C under N_2 atmosphere resulted in production of a black melt. This reaction mixture was separated by monitoring green fluorescence of a tribenzosubporphine. Repeated separations over silica gel column provided B(III)–tribenzosubporphine **2-OH**. Alternatively, microwave irradiation of the same solid mixture gave a similar melt that contained **2-OH**. Although the yield was quite low (up to 1.4%), the reproducibility of this reaction is high.[137]

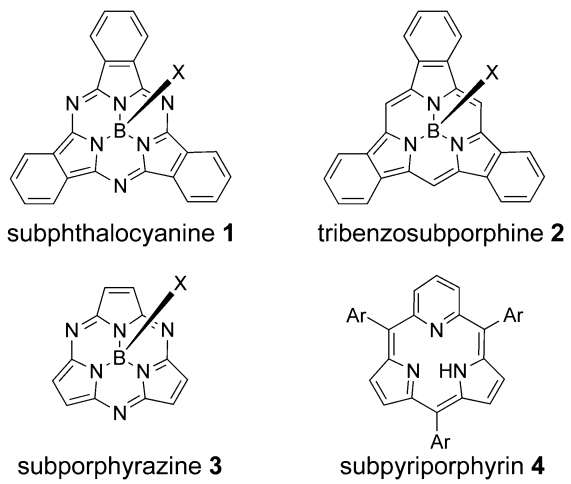

Figure 1. Subphthalocyanine and subporphyrin analogs.

The hydroxy group axially coordinated at the boron atom of **2-OH** can be easily replaced by an alkoxy group by simple heating in an alcohol solution. B–methoxy and B–isopropoxy coordinated tribenzosubporphines **2-OMe** and **2-O*i*-Pr** were thus readily prepared (Scheme 2). These facile ligand exchange reactions are in sharp contrast to those of subphthalocyanines.[139] The equilibrium was observed between **2-OH** and **2-OCOCF$_3$** or **2-OCOPh** in the presence of carboxylic acid. For example, the equilibrium constant between **2-OH** and **2-OCOPh** was determined by ^{1}H NMR titration to be $K = 3.2$. Thus, subporphines **2-OCOPh** and **2-OCOCF$_3$** were prepared by continuous removal of water from a solution of **2-OH** and a corresponding carboxylic acid.[137] Since the methoxy-coordinated subporphine **2-OMe** is most stable on a silica gel column, subporphines have been usually isolated and characterized as their B–methoxy-coordinated forms.

X-ray crystallographic analysis revealed that the structures of tribenzosubporphines **2-OH**, **2-OMe**, **2-O*i*-Pr**, and **2-OCOCF$_3$** are all bowl-shaped triangular skeletons. A typical example is represented for **2-OH** in Figure 2. The central boron atom was placed in the tripyrrolic pocket with N–B distances of 1.477–1.513 Å in a tetrahedral fashion, and B–O bond lengths are in 1.435–1.545 Å. The degree of macrocyclic curvature can be characterized by "bowl-depth" that is defined as the distance from the boron atom to the mean plane of peripheral six benzocarbons; 2.33 Å for **2-OH**, 1.70 Å for **2-OMe**, 2.10 Å for **2-O*i*-Pr**, and 2.02 Å for **2-OCOCF$_3$**. Typically, the ^{1}H NMR spectrum of **2-OH** exhibits a simple pattern consisting of a singlet at 9.44 ppm due to the *meso*-protons, a pair of double doublets at 8.86 and 7.88 ppm due to the benzo-protons, and a broad signal at −2.60 ppm due to the axial-OH proton. The ^{11}B NMR spectrum exhibits a singlet peak at −14.6 ppm, which is slightly less shielded in comparison to those of subphthalocyanines that appear in the range of −17.7 to −19.6 ppm.[139] Other tribenzosubporphines exhibit similar ^{1}H and ^{11}B NMR spectra.[137] These data allowed us to conclude a diatropic ring current, and thus aromaticity for tribenzosubporphine **2** arising from 14π-aromatic circuit despite the substantially bent structures.

Just after our first synthesis of tribenzosubporphines, Latos-Grażyński et al. reported in a paper on subpyriporphyrin **4**,[143] a core-modified, pyridine-embedded subporphyrin analog, which

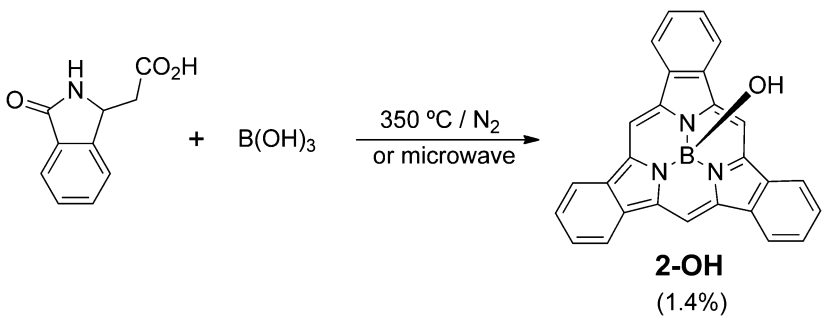

Scheme 1. Synthesis of tribenzosubporphine **2-OH**.

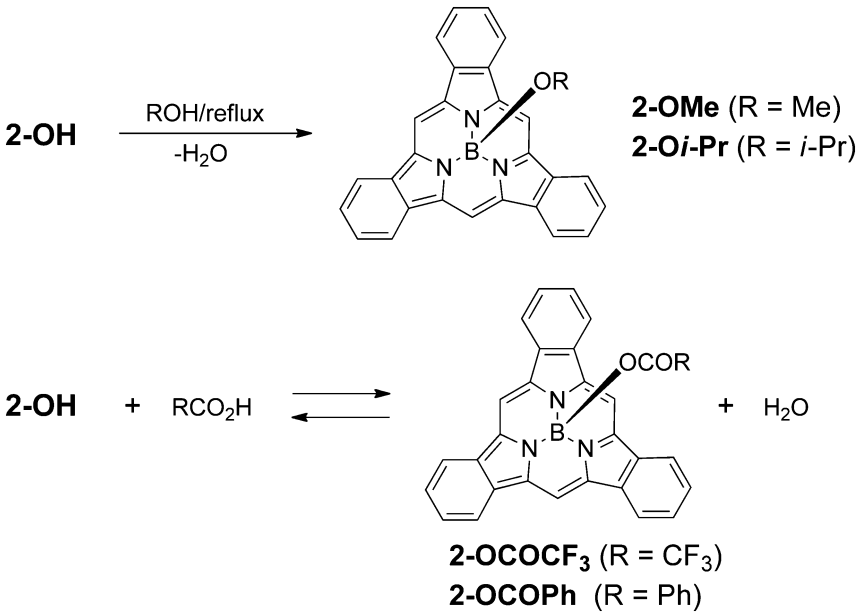

Scheme 2. Axial ligand exchange reactions.

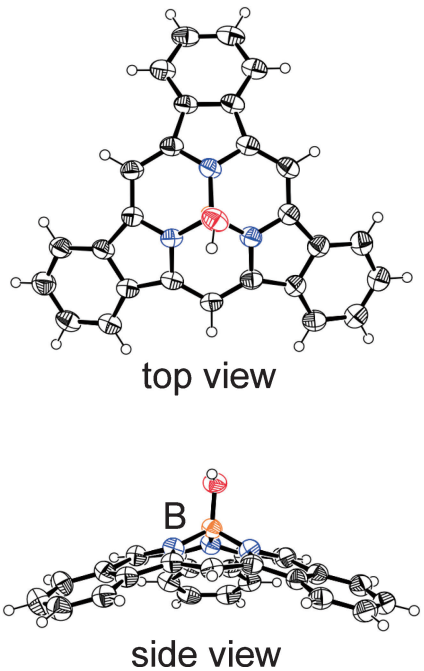

Figure 2. Crystal structure of **2-OH**.

existed as a free-base form without the boron center. It is believed that the replacement of a pyrrole ring by a pyridine ring is favorable for the stabilization of a free-base form owing to mitigation of steric repulsion between the inner NH hydrogen atoms. Besides this example, several ring-contracted porphyrins were reported.[144]

2.3 *meso*-Aryl-Substituted Subporphyrins. *meso*-Aryl-substituted subporphyrins were first reported by Kobayashi and co-workers in 2007.[145a] They synthesized *meso*-aryl-substituted subporphyrins from tri-1-pyrrolylborane (**5**) and aryl aldehyde in propionic acid by refluxing. Yields of subporphyrins were reported to be 4–8%. Shortly after, our group reported more reliable synthetic protocols using 1-(tri-1-pyrrolylboryl)pyridine (**6**) as a more stable precursor toward moisture and air (Figure 3).[146] A suspension of **6** and 3 equiv of aromatic aldehyde in *o*-dichlorobenzene was treated with TFA at 0 °C. After quenching the acid catalyst, the resulting solution was refluxed under aerobic conditions to provide *meso*-aryl subporphyrins in up to 5.6% yield (Scheme 3). This protocol is effective for most of the aryl aldehydes examined with the exception of *ortho*-substituted aromatic aldehydes. For such sterically hindered substrates, rather harsh Adler-type conditions were required to produce subporphyrins.[145]

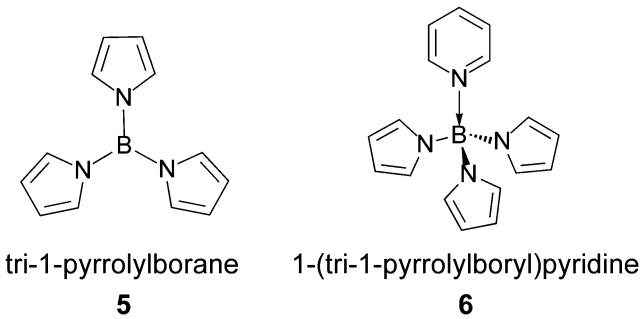

Figure 3. Tri-1-pyrrolylboranes.

X-ray diffraction analysis revealed that the solid-state structures of **7**, **8**, **9-OCOCF$_3$** (axial ligand is –OCOCF$_3$), **10**, **11**, and **12** are all bowl-shaped bent conformations with bowl-depths of 1.18–1.41 Å (Figure 4). Interestingly, the dihedral angles between *meso*-aryl ring and subporphyrin core for *ortho*-free subporphyrins **7**–**11** in the solid-state are variable in a range of 38.3–55.7°. These dihedral angles are notably smaller than those of porphyrins that are generally larger than 60°. On the other hand, 2,4,6-trimethoxyphenyl-substituted subporphyrin **12** exhibits larger dihedral angles of 68.7–75.7°. In line with these structural differences, ^{1}H NMR spectroscopy revealed marked differences in rotational barriers between **12** and **13**. Signals due to the two *ortho*-protons of the 3,4,5-trimethoxyphenyl substituent in **13** are observed as a singlet even at −90 °C in CD_2Cl_2, indicating a free rotation of the

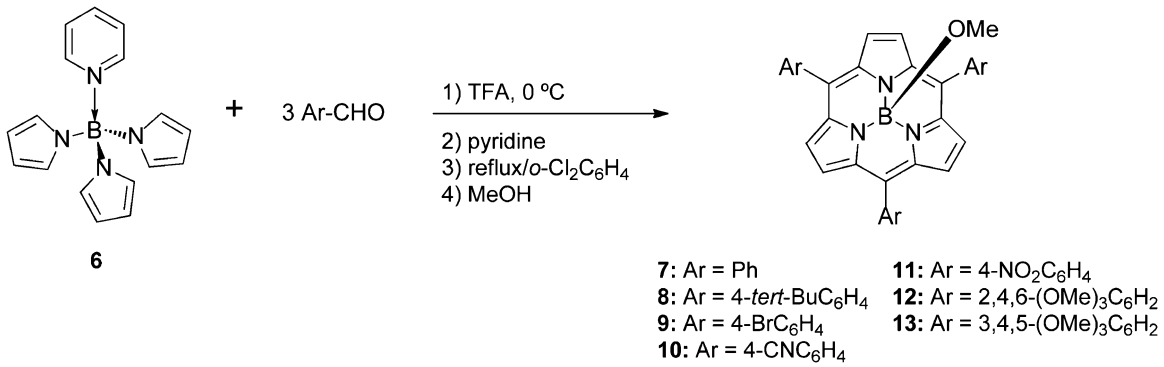

Scheme 3. Synthesis of *meso*-aryl-substituted subporphyrins.

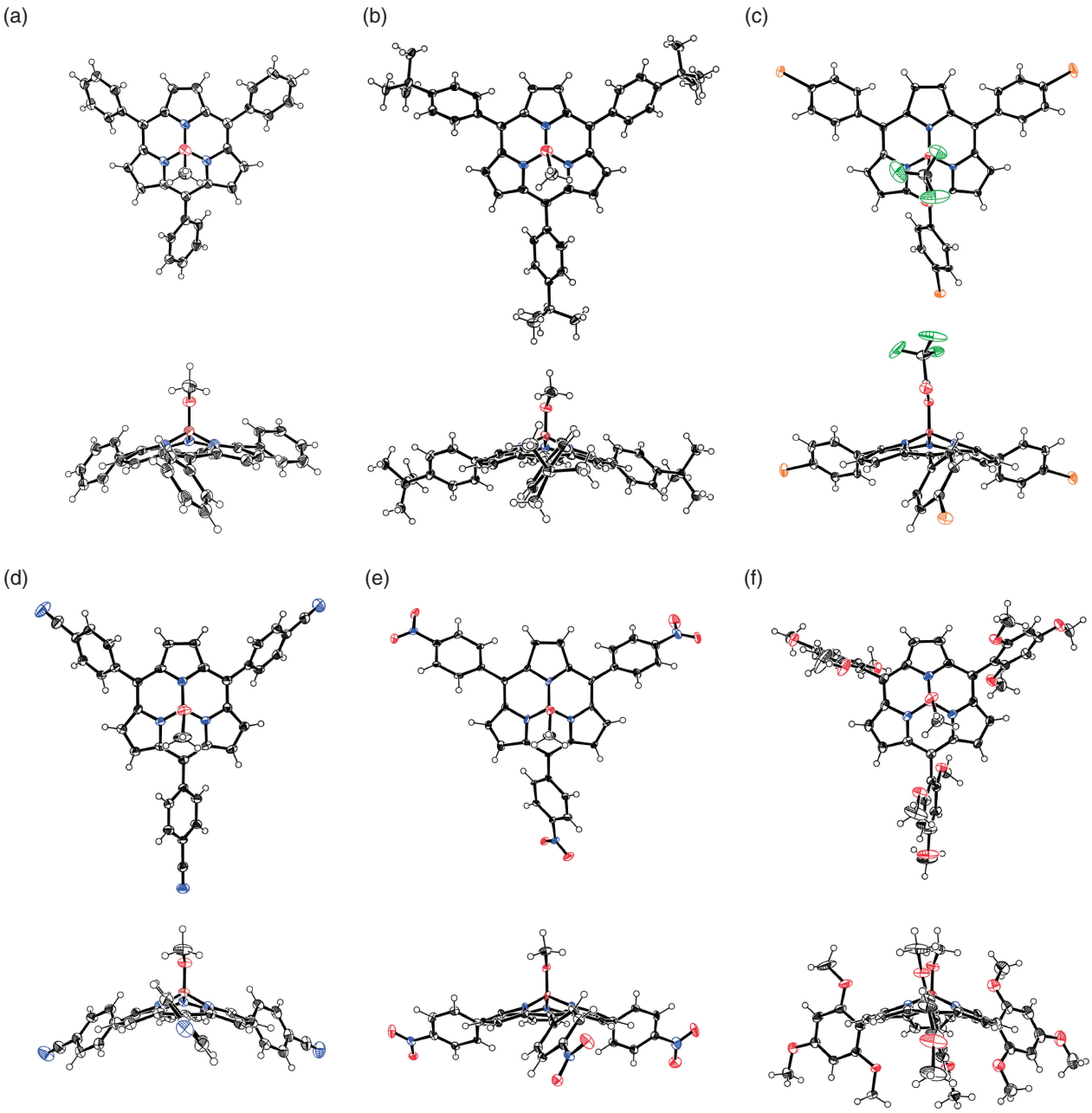

Figure 4. Crystal structures of (a) **7**, (b) **8**, (c) **9-OCOCF$_3$**, (d) **10**, (e) **11**, and (f) **12**.

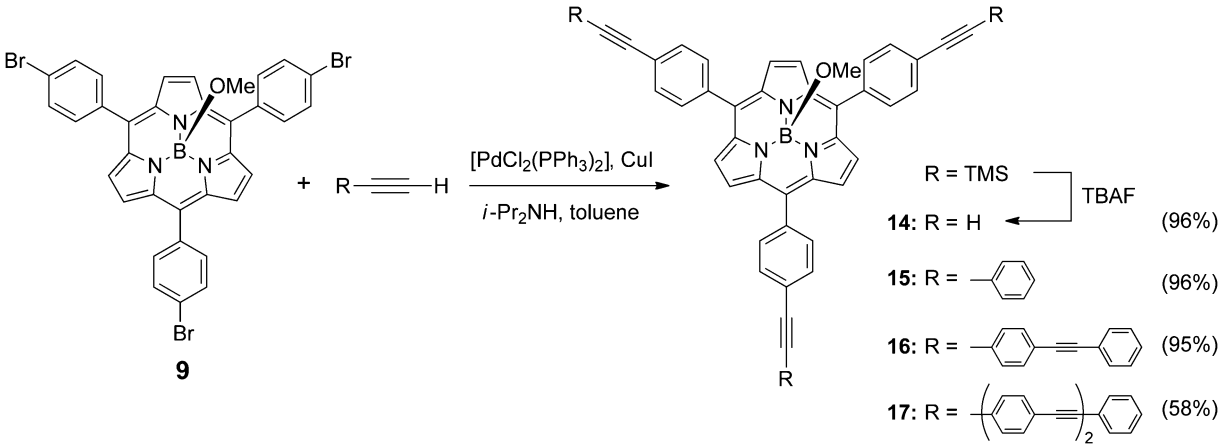

Scheme 4. Synthesis of subporphyrins **14**–**17** (TBAF: tetrabutylammonium fluoride).

meso-aryl substituents. On the other hand, the two *meta*-protons of 2,4,6-trimethoxyphenyl groups in **12** resonate differently at 6.50 and 6.32 ppm and the two *ortho*-methoxy protons also resonate differently at 3.79 and 3.32 ppm, and these signals do not coalesce even at 130 °C in tetrachloroethane-d_2. Thus, the rotation of 2,4,6-trimethoxyphenyl substituents in **12** has been concluded to be sterically blocked.

The free rotational characteristics of sterically unhindered *meso*-aryl substituents are expected to lead to large substituent effects on the electronic properties of subporphyrins. This is indeed the case. In the UV–vis absorption spectra, subporphyrins **7**–**10** and **13**, which bear sterically unhindered *meso*-aryl substituents, exhibit absorption and fluorescence spectra essentially similar to those of **8** that display an intense Soret-band at 377 nm and two Q-bands at 465 and 491 nm, and green fluorescence at 516 nm with a quantum yield of $\Phi_F = 0.16$. On the other hand, subporphyrin **12** that bears sterically hindered *meso*-aryl substituents shows a distinctly different absorption spectrum that contains a Q-band at 454 nm and blue-shifted fluorescence. The most notable example is 4-nitrophenyl-substituted subporphyrin **11** that exhibits absorption and fluorescence spectra indicative of intramolecular charge-transfer interaction. This can be explained in terms of low-lying LUMO levels of *meso*-attached nitrobenzene moieties and large interaction of *meso*-substituents with subporphyrin core through π-conjugation.[146]

2.4 *meso*-Oligo(1,4-phenyleneethynylene)-Substituted Subporphyrins. Scheme 4 outlines the synthetic routes to **14**, **15**, **16**, and **17**. Sonogashira coupling reactions of 4-bromophenyl-substituted subporphyrin **9-OMe** with trimethylsilylacetylene, phenylacetylene, and 4-(phenylethynyl)phenylacetylene gave **14**, **15**, and **16** in 96, 96, and 95%, yields respectively.[146] It is worth to note that subporphyrins **14**–**16** are readily soluble in CH_2Cl_2, $CHCl_3$, and toluene despite the presence of three oligo(1,4-phenyleneethynylene) units without any bulky substituents. The yield of **17** was only 58%, probably due to the poor solubility of the acetylene precursor. Subporphyrins **14**–**17** exhibit similar ^{1}H NMR spectral patterns, featuring a singlet in the range of 8.12–8.17 ppm due to the peripheral β-protons and a single set of signals without discrimination of the two phenylene protons at the 2,6- or 3,5-positions due to the 1,4-phenyleneethynylene groups. These

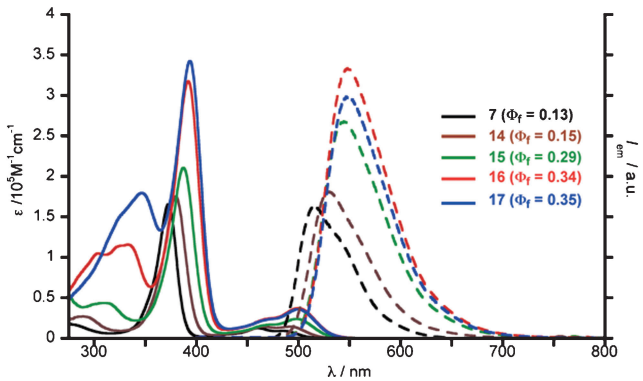

Figure 5. UV–vis absorption (solid lines) and fluorescence (dashed lines) spectra of subporphyrins **7** and **14**–**17** in CH_2Cl_2.

^{1}H NMR data indicate the C_3-symmetry for the subporphyrins **14**–**17** and free rotation of the *meso*-aryl substituents. Upon elongation of the *meso*-oligo(1,4-phenyleneethynylene)s chain length, the Soret- and Q-bands are red-shifted with a progressive intensification (Figure 5). While the Q(1,0) band is more intense than the Q(0,0) band in the case of **7**, the relative intensity of Q(0,0) band progressively increases upon elongation of substituted 1,4-phenyleneethynylene chains. These spectral changes reveal the electronic interactions between subporphyrin core and *meso*-oligo(phenyleneethynylene) chains, however it reaches a saturation point at the stage of **16**, beyond that no significant spectral change occurs. Since the natural radiative lifetime (τ_0) is expected to have a correlation with the actual radiative size of the chromophore and fluorescence lifetime, the natural radiative rate constants were calculated from the fluorescence quantum yield and fluorescence lifetime according to the relationship of ($k_r = 1/\tau_0$, $\tau_0 = \tau_f/\Phi_f$) to be 5.5×10^7, 7.5×10^7, 1.5×10^8, 1.9×10^8, and $2.2 \times 10^8\ s^{-1}$ for **7**, **14**, **15**, **16**, and **17**, respectively, in agreement with the increasing size of the effective radiative chromophore with the elongation of *meso*-oligo(1,4-phenyleneethynylene)s substituents.

2.5 *meso*-[4-(Dialkylamino)phenyl]-Substituted Subporphyrins. Subporphyrins **18**–**20** were prepared by means of palladium-catalyzed Buchwald–Hartwig amination protocol[147] from corresponding 4-bromophenyl-substituted subporphyrins

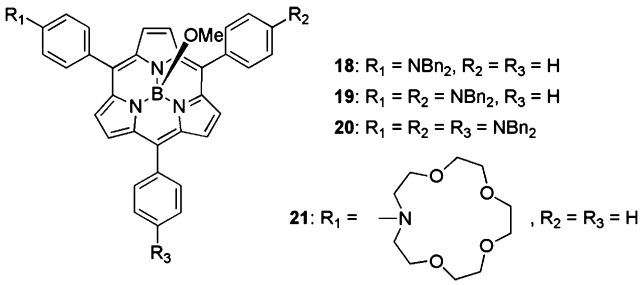

Figure 6. *meso*-[4-(*N*,*N*-Dialkylamino)phenyl]-substituted subporphyrins (Bn: benzyl).

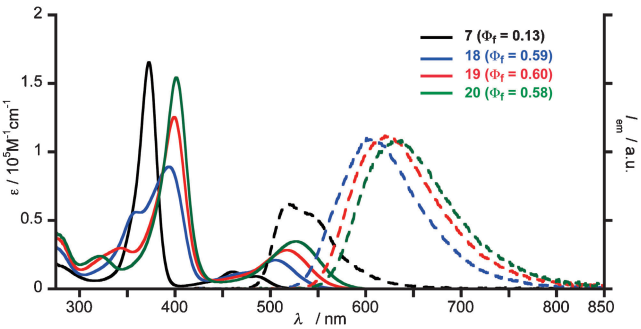

Figure 7. UV–vis absorption (solid lines) and fluorescence (dashed lines) spectra of **7** and **18**–**20** in CH_2Cl_2.

and dibenzylamine (Figure 6).[148] The solid-state structures of **18** and **20-OEt**, a B–OEt analog of **20**, revealed that each 4-aminophenyl group exhibits slight but distinct distortion toward a quinodimethene-like form. Namely, the bond lengths of C2–C3 and C5–C6 are shorter than the other bonds in the 4-aminophenyl substituent in **18** and all the 4-aminophenyl substituents in **20**. The UV–vis absorption spectra of **18**–**20** are clearly different depending on the number of 4-aminophenyl substituents (Figure 7). Subporphyrin **18** exhibits a split Soret-band at 359 and 394 nm and a red-shifted Q-like band at 505 nm compared to that of triphenylsubporphyrin **7**. Subporphyrin **19** also displays a split Soret band but its shape is changed; a high-energy band at 343 nm is attenuated and a low-energy band at 401 nm is intensified. Interestingly, subporphyrin **20** shows a nonsplit sharp Soret-band at 401 nm. These spectral changes in the Soret-band underscore the characteristic substituent effects of subporphyrin. The calculations also indicate that HOMOs of **18**–**20** are progressively destabilized in this order through the orbital interactions with dimethylaminophenyl moiety, which is in good agreement with the first oxidation potentials measured by cyclic voltammetry; **18** (0.38 V), **19** (0.30 V), **20** (0.26 V), and **7** (0.71 V). Subporphyrins **18**–**20** emit reddish-orange fluorescence tailing over 800 nm as mirror images of their Q-like bands. Remarkably, the fluorescence quantum yields of **18**–**20** recorded in CH_2Cl_2 are drastically enhanced; $\Phi_F = 59$, 60, and 58%, respectively, which are more than fourfold of that of **7** ($\Phi_F = 13\%$) (Figure 8). The fluorescence lifetimes of **18**–**20** determined by time-correlated single photon counting method are considerably longer than those of **7** in solvents examined, hence suggesting suppression of nonradiative decaying route in the singlet excited-state. These subporphyrins **18**–**20** also exhibit solvatochromic behaviors in the absorption and fluorescence

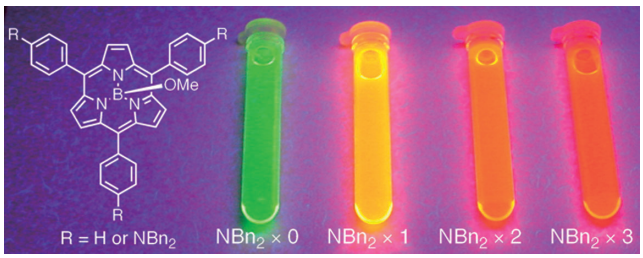

Figure 8. Fluorescence of subporphyrins **7** and **18**–**20**.

spectra. Strong electronic interaction between the 4-aminophenyl substituent and the subporphyrin core is attractive in view of chemical sensing system. Along this line, aza-crown-substituted subporphyrin **21** was designed and prepared via the similar Pd-catalyzed amination route. Similarly to **18**, the subporphyrin **21** shows a split Soret-band at 358 and 394 nm, and Q-band at 508 nm in acetonitrile due to electron-donating character of the nitrogen atom embedded in the crown ether. Cation binding ability of **21** was examined by UV–vis absorption and fluorescence titration in acetonitrile using perchlorate salts. Upon addition of $Ca(ClO_4)_2$, the perturbed absorption spectrum of **21** gradually changed to an unperturbed one that was quite similar to that of triphenylsubporphyrin **7** with several clear isosbestic points, allowing accurate determination of the binding constants. This Ca^{2+} binding can be monitored by a vivid color change of solution from orange to yellow. During the titration, the perturbed reddish-yellow fluorescence of **21** changed to normal subporphyrin-like green-yellow fluorescence. Similar binding events were confirmed with other metal cations.[148] As an advantageous feature, the fluorescence spectra of solutions of cation-bound **21** were found to vary among orange, yellow, and green, depending upon binding cation.

2.6 Capped Subporphyrins. Capped subporphyrins **22**–**26** with C_3 molecular symmetry were synthesized from 5,10,15-tri(3-aminophenyl)-substituted subporphyrin **27** and tripodal trialdehydes **28**–**32** via Lindsey's entropically favored macrocyclization (Scheme 5).[149,150] X-ray diffraction analysis has revealed that the concave surface of subporphyrin core is selectively capped with a 1,3,5-substituted benzene moiety. Capped subporphyrins **25** and **26** possessing 5-atom arm-length and thus large inner cavities exhibit solvent incorporation behaviors in their crystal structures. On the other hand, subporphyrins **22** and **23** exhibit tight structures, where the cap and subporphyrin core are found much closer with averaged interplanar separations of 3.56 and 3.15 Å, respectively. Variable-temperature ^{1}H NMR measurements revealed that subporphyrins **22**, **23**, and **26** undergo spiral interconversions between *P*- and *M*-forms depending on the arm length and the electronic nature of the cap. Of these, subporphyrin **23** bearing a 1,3,5-tris(alkoxycarbonyl)benzene cap strapped by 3-atom arms exhibits a considerably slow spiral interconversion with a large enthalpy change of $\Delta H^{\ddagger} = 76.4\,\mathrm{kJ\,mol^{-1}}$ and characteristic red shift of Soret-like band and enhancement of Q(0,0) band. These properties are ascribed to considerable through-space charge-transfer interactions between the electron-deficient cap and the subporphyrin core and the multiple CH–π interactions.

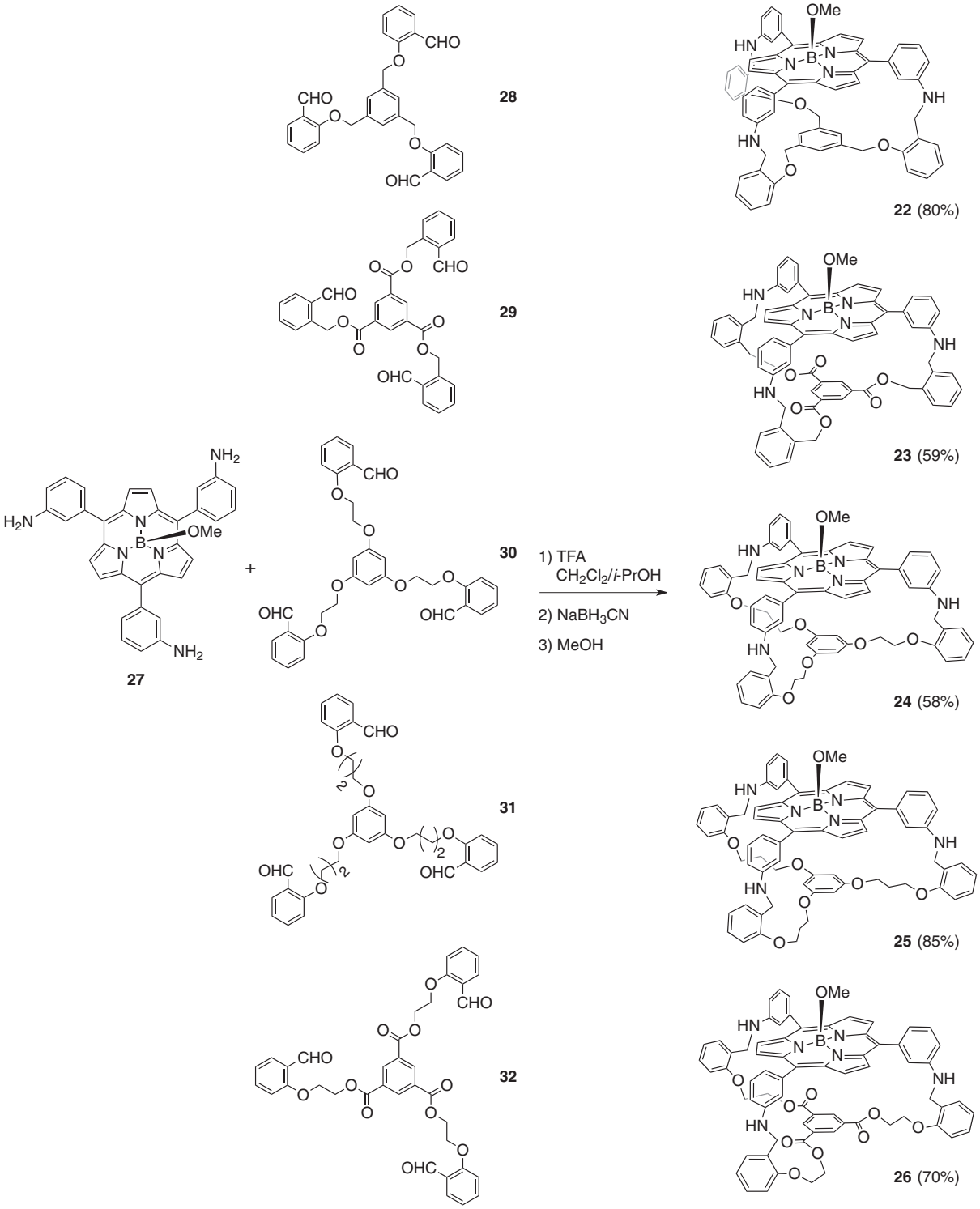

Scheme 5. Capped subporphyrins.

2.7 Hybrid Systems with Various Functional Molecules. Porphyrin–subporphyrin hybrids **33**–**35** were prepared by Suzuki–Miyaura coupling of tris(4-bromophenyl)subporphyrin **9** with 5-pinacolate borylporphyrin followed by reduction of unreacted bromo groups (Figure 9). In these hybrids, the fluorescence of the subporphyrin moiety is completely quenched, indicating the efficient excitation energy transfer from the subporphyrin segment to the porphyrin segment.[151]

BODIPY–subporphyrin hybrids bridged by a 1,4-biphenylene or 1,4-diphenylethynylene spacer were synthesized either by palladium-catalyzed Suzuki–Miyaura reaction or Sonogashira reaction (Figure 10).[152] In all cases, intramolecular excitation energy transfer from the subporphyrin core to the BODIPY peripheries is efficient, but the fluorescence intensity of the BODIPY segments is found to depend upon the presence or absence of β-methyl groups of the BODIPY subunit.

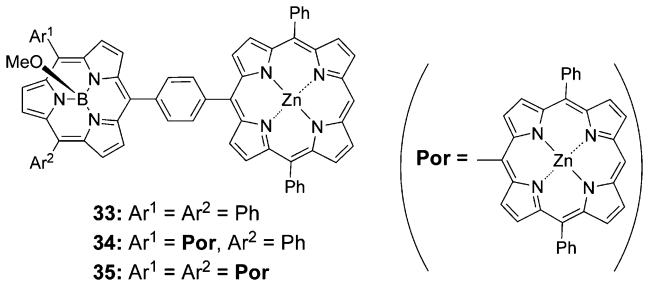

Figure 9. Porphyrin–subporphyrin hybrids.

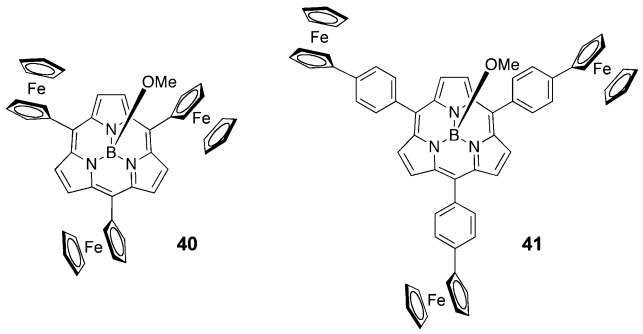

Figure 11. Ferrocene-appended subporphyrins.

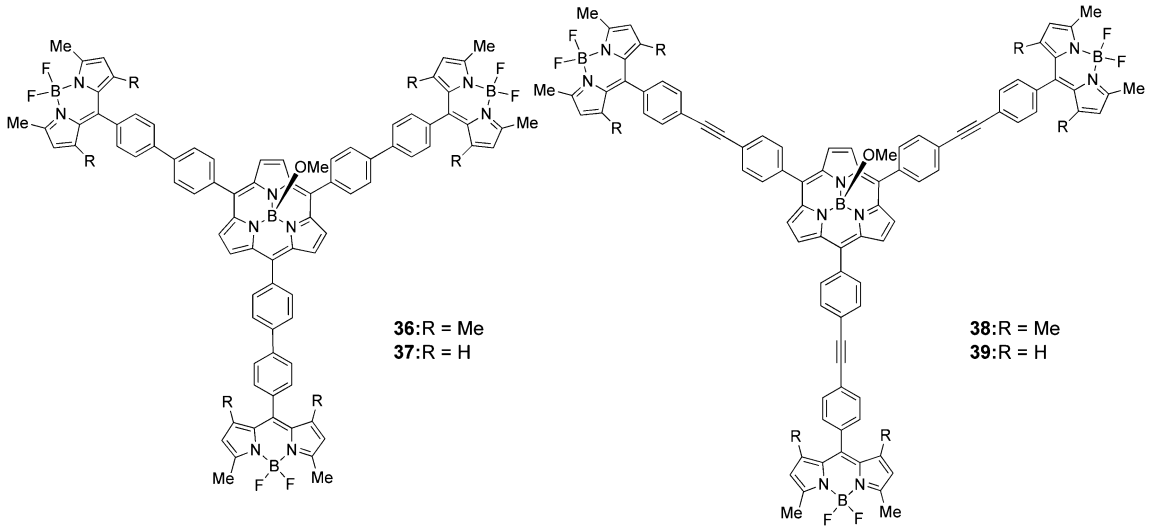

Figure 10. BODIPY–subporphyrin hybrids.

Ferrocene-appended subporphyrins **40** and **41** were prepared by conventional acid-catalyzed condensation and Suzuki–Miyaura cross-coupling, respectively (Figure 11).[153] Both subporphyrins showed red-shifted absorption spectra and strong fluorescence quenching. Subporphyrin **40** displayed split first oxidation potential with $\Delta E = 168$ mV, while **41** exhibited the corresponding nonsplit potential. These data indicate the effective and negligible electronic communication among the ferrocene moieties for **40** and **41**, respectively.

meso-Thienyl-substituted subporphyrin **42**, which was prepared by the standard protocol, was brominated with *N*-bromosuccinimide selectively at the thienyl α-position to give **43**. Suzuki–Miyaura coupling of **43** with oligothienyl boronic acids gave *meso*-oligothienyl-substituted subporphyrins **44**, **45**, and **46** (Scheme 6).[154] With increasing number of thienylene subunits, the Soret-like bands are red-shifted and intensified continuously with peak positions of 394, 420, 436, and 446 nm, while the Q-like bands were observed in the same manner at 522, 557, 572, and 575 nm, respectively. Along these changes, the fluorescence spectra are also red-shifted with peak positions of 603, 680, 714, and 727 nm, respectively. These spectral changes reveal the effective electronic interactions between the subporphyrin core and *meso*-oligothienylene chains. Interestingly, the fluorescence quantum yields are high for **42** ($\Phi_f = 0.35$) and **44** ($\Phi_f = 0.33$) but are dropped for **45** ($\Phi_f = 0.17$) and **46** ($\Phi_f = 0.16$). It is worth noting that the

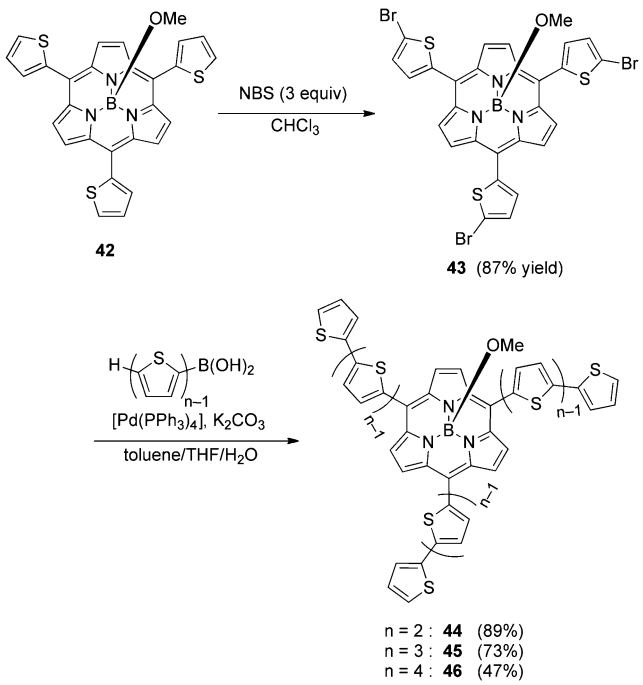

Scheme 6. Synthesis of *meso*-oligothienylsubporphyrins.

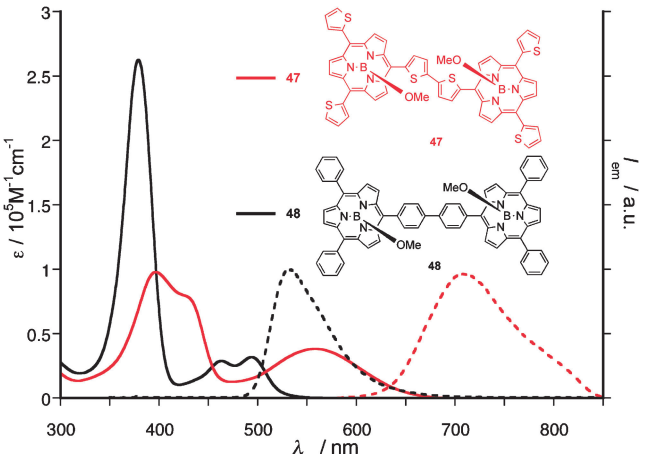

Figure 12. UV–vis absorption (solid lines) and fluorescence (dashed lines) spectra of dimeric subporphyrins **47** and **48** in CH_2Cl_2.

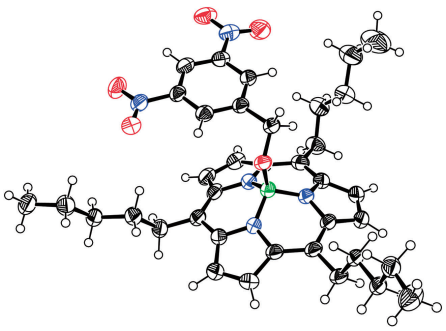

Figure 13. Crystal structure of **52-DN**.

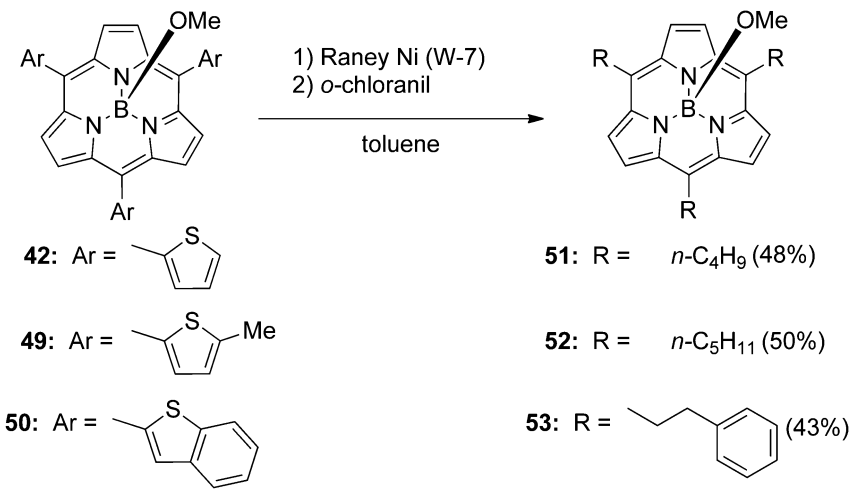

Scheme 7. Synthesis of trialkylsubporphyrins.

optical properties of **45** and **46** are rather similar, suggesting saturation for oligothienylene conjugation.

A dimeric subporphyrin **47** exhibits a split Soret-like band due to the exciton coupling and considerably red-shifted and broad Q-like band, compared with biphenylene-bridged subporphyrin **48** (Figure 12).[155]

2.8 *meso*-Alkyl-Substituted Subporphyrins. In the next step, we attempted the synthesis of *meso*-alkyl-substituted subporphyrins. Acid-catalyzed condensation reactions of **6** and aliphatic aldehydes were extensively examined under various conditions, but all these attempts failed. We envisioned that Raney nickel reduction of *meso*-thienyl-substituted subporphyrins would provide *meso*-alkyl-substituted subporphyrins via reductive desulfurization. Subporphyrins **42**, **49**, and **50** were prepared by the conventional method in 1.7%, 3.7%, and 0.9% yields, respectively (Scheme 7).[156] A toluene solution of **49** was treated with W-7 Raney nickel at 40 °C for 30 min and TLC analysis confirmed the consumption of **49**. The ^{1}H and ^{11}B NMR spectra of the reaction mixture indicated the formation of *meso*-tripentylsubporphyrin **52** along with several over-reduced products. Since these reduction products were difficult to separate, the reaction mixture was once oxidized with *o*-chloranil to give a simple mixture, from which **52** was isolated in 50% yield. In the same manner, *meso*-tributylsubporphyrin **51** and *meso*-tris(2-phenylethyl)subporphyrin **53** were obtained in 48 and 43% yields, respectively. Subporphyrins **51**–**53** are quite soluble in organic solvents including methanol and hexane, hence making their crystallization rather difficult. Fortunately, nice crystals were obtained by slow recrystallization of an ether solution of 3,5-dinitrobenzylsubporphyrin **52-DN** that was prepared by refluxing a toluene solution of **52** in the presence of 3,5-dinitrobenzyl alcohol. The crystal structure of **52-DN** displays a bowl-shaped C_3-symmetric structure with a bowl depth of 1.37 Å (Figure 13). The UV–vis absorption spectrum of **52** in CH_2Cl_2 exhibits Soret-like bands at 360 nm with a shoulder at 344 nm and Q-like bands at 450 and 472 nm, which are both blue-shifted and more intensified than those of **7** (Figure 14). Importantly, comparison of the optical data of **52** and **7** reveals a substantial electronic conjugation of the *meso*-phenyl groups to the subporphyrin core, which are only marginal for porphyrins. It is worthy to note that the absorption spectrum of **52** indicates clear vibronic structures for the Soret-like band as well as the Q-like bands that are reminiscent of the absorption features of

typical porphyrins. The steady state fluorescence spectrum of **52** also exhibits a vibronic structure with peaks at 476 and 507 nm in a mirror image of the Q-like band spectrum. The small Stokes shift value (489 cm^{-1}) reflects the rigid structure of subporphyrin core in **52**, because the radiative part of the chromophore has been limited to the core alone. The fluorescence quantum yield of **52** was also determined to be small, being 0.07. The fluorescence lifetime of **52** was measured to be 3.2 ns, and the natural radiative rate constant was calculated to be $2.2 \times 10^7\ s^{-1}$. The larger radiative rate of **7** than that of **52** underscores that the intrinsic photophysical properties of subporphyrins are influenced remarkably by conjugated interactions with *meso*-aryl substituents

2.9 Subchlorins. In the synthesis of *meso*-triphenylsubporphyrin **7**, a reddish-orange band always eluted closely with a yellow band of **7**. After repeated separations over silica gel columns, this side product was isolated and identified as subchlorin **55**.[157] The formation of subchlorin is reminiscent of the formation of chlorin in the well known Adler–Longo synthesis of tetraphenylporphyrins (TPP).[158] Subchlorin, a ring-contracted congener of chlorin, has a 14π-conjugated aromatic macrocycle which is essentially the same as that of subporphyrin as shown in Scheme 8. Since one β–β double bond is reduced in **55**, the symmetry of subchlorin (C_s) is lower than that of subporphyrin (C_{3v}). We found that *meso*-aryl subporphyrins **7**, **54**, and **12** underwent hydrogenation at one β–β double bond upon treatment with *p*-toluenesulfonohydrazide under basic conditions to give subchlorins **55**, **56**, and **57** in 34, 24, and 36% yields, respectively. Subchlorins **55**–**57** were oxidized back to subporphyrins **7**, **54**, and **12** quantitatively upon treatment with MnO_2. On the basis of these results, we improved our synthetic method of subporphyrin by adding MnO_2 oxidation procedure for the conversion of **55** to **7** before separation. This indeed facilitated the separation step and improved the yield of subporphyrin **7** to 6.3% from 3.9%.

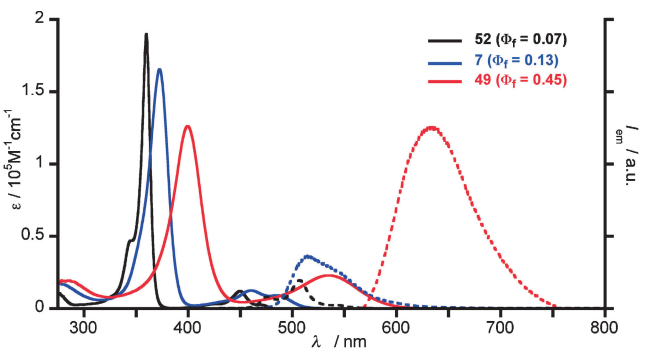

Figure 14. UV–vis absorption (solid lines) and fluorescence (dashed lines) spectra of **52** (black), **7** (blue), and **49** (red) in CH_2Cl_2.

In the crystal structure of **56**, the bond length of a β–β single bond is 1.501 Å, which is significantly longer than those of β–β double bonds (1.420 and 1.421 Å; Figures 4 and 16a). The ^{1}H NMR spectrum of **56** exhibits a couple of doublets at 7.85 and 7.50 ppm due to β-C(sp^2)–H protons, and double doublets in the range of 4.19–3.47 ppm due to the methylene β-protons along with two sets of proton signals due to the *meso*-aryl groups. Importantly, the axial methoxy protons and the central boron atom of **56** appear at 1.54 and −12.1 ppm in its ^{1}H and ^{11}B NMR spectra, indicating a diatropic ring current, which is slightly weaker than that of subporphyrin **54**.

The UV–vis absorption spectrum of **54** shows a sharp Soret-like band at 377 nm and weak Q-like bands at 464 and 492 nm, whereas subchlorin **56** exhibits a less intense and blue-shifted Soret-like band at 333 nm and intensified and red-shifted Q-like bands at 458 and 529 nm. Fluorescence emission of **56** was observed at 552 nm as a mirror image of a Q-like band, which tailed over 700 nm. Effects of *meso*-aryl substituents are also observed for subchlorins, in that *meso*-2,4,6-trimethoxyphenyl-substituted subchlorin **57** shows a split Soret-like band at 311 and 326 nm and fluorescence at 544 nm as a much sharper spectrum as compared with **56**.

2.10 Subbacteriochlorins. Hydrogenation of *meso*-triphenylsubporphyrin **7** with Raney nickel furnished *meso*-aryl-substituted subbacteriochlorin **58** in 47% yields (Figure 15).[159] It is worthy to note that any further reduction over subbacteriochlorin has not been detected. Quick separation over silica gel column is critical for the isolation of pure subbacteriochlorin due to feasibility toward oxidation. Slow recrystallization from a mixture of acetonitrile and heptane provided nice crystals of **58-OEt** that was easily prepared by heating of **58** in the presence of ethanol. Single-crystal X-ray diffraction analysis revealed that **58-OEt** has a nonsymmetric structure with two β–β single bonds of 1.486 and 1.511 Å and a β–β double bond of 1.425 Å and a bowl-depth of 1.26 Å (Figure 16). Importantly, the fluorescence of **58** is remarkably intensified ($\Phi_F = 0.42$) at 550 nm, which is distinctly red-shifted from **7** (520 nm, $\Phi_F = 0.13$) or slightly blue-shifted

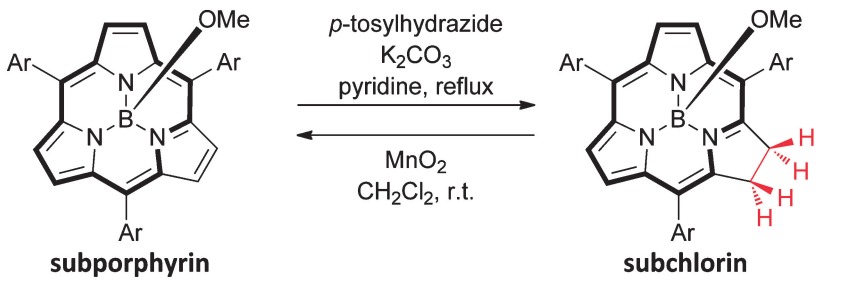

7: Ar = Ph
54: Ar = 3,5-*tert*-$Bu_2C_6H_3$
12: Ar = 2,4,6-$(OMe)_3C_6H_2$

55: Ar = Ph
56: Ar = 3,5-*tert*-$Bu_2C_6H_3$
57: Ar = 2,4,6-$(OMe)_3C_6H_2$

Scheme 8. Interconversion between subporphyrins and subchlorins.

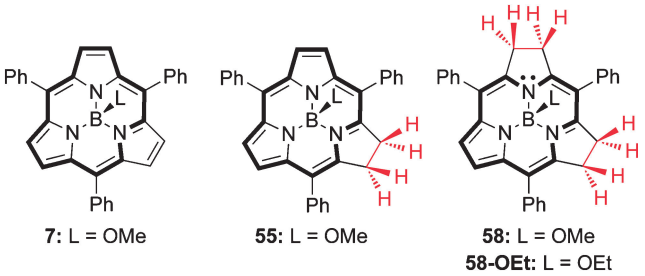

Figure 15. Subporphyrin **7**, subchlorin **55**, and subbacteriochlorin **58** (14π-Electronic circuits are indicated in black bold lines.).

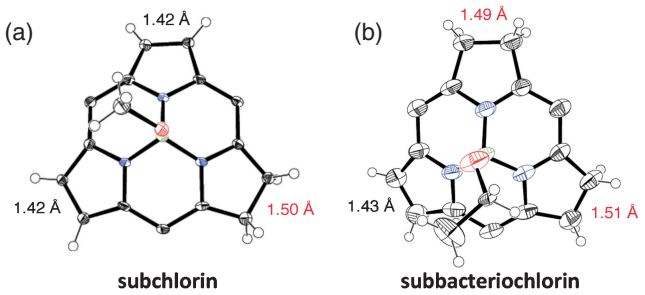

Figure 16. Crystal structures of (a) **56** and (b) **58-OEt** (*meso*-Aryl groups are omitted.).

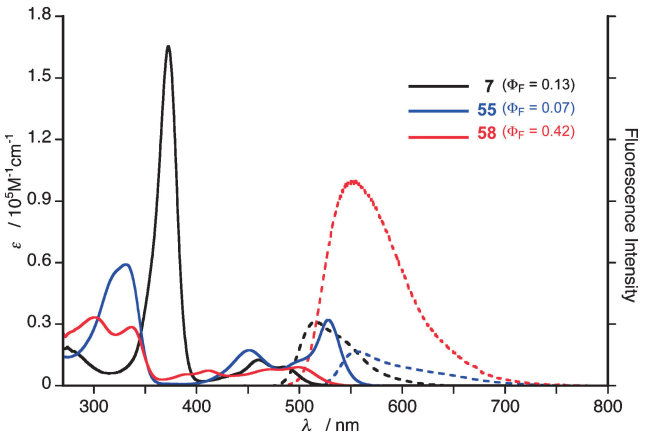

Figure 17. UV–vis absorption (solid lines) and fluorescence (dashed lines) spectra of subporphyrin **7** (black), subchlorin **55** (blue), and subbacteriochlorin **58** (red) in CH_2Cl_2.

from **55** (556 nm, $\Phi_F = 0.07$) (Figure 17). The high fluorescence quantum yield of **58** has been ascribed to the slower nonradiative decay, since the radiative decay rates are similar for **7**, **55**, and **58**. Collectively, subbacteriochlorins are modestly aromatic because of the 14π-electronic circuit that involves the lone pair electrons of nitrogen atom and exhibit characteristic blue-shifted Soret-like bands, red-shifted Q-like bands, enhanced fluorescence, and high oxidation potentials.

Importantly **58** was found to be smoothly and selectively oxidized to **55** with Ag_2O in 86% yield. Therefore, the initial reduction of subporphyrin to subbacteriochlorin followed by oxidation with Ag_2O constitutes a novel synthetic route to subchlorins. This stepwise synthesis is superior to the reduction of **7** with *p*-tosylhydrazide previously reported by us.[157] Actually, subchlorin **55** was prepared in 74% from **7** via this two-step route without isolation of unstable **58**.

Comparison of the properties of subporphyrin **7**, subchlorin **55**, and subbacteriochlorin **58** is important. The B-axial methoxy protons resonate at 0.82, 1.51, and 2.34 ppm, and the central boron resonates at −15.3, −12.1, and −8.0 ppm for **7**, **55**, and **58**, respectively, indicating the decreasing diatropic ring current and hence the aromaticity in the order of **7** > **55** > **58**. In line with this trend, the nuclear independent chemical shifts (NICS) values have been calculated at B3LYP/6-311G(d) level to be −18.9, −14.9, and −10.9 ppm, respectively.

2.11 Peripheral Modifications. Peripheral modifications of *meso*-aryl-substituted subporphyrins were performed as follows. First, perbromination of **54** proceeded nearly quantitatively by the reaction with molecular bromine to give **59**. Suzuki–Miyaura coupling of **59** with phenylboronic acid gave hexaphenylated subporphyrin **60** in 73% yield. Similarly, Stille coupling with trimethyl(phenylethynyl)tin(IV) gave hexakis-(phenylethynyl)-substituted subporphyrin **61** in 89% yield. The structures of **59**, **60**, and **61** were determined by X-ray diffraction analysis (Figure 18).[160] The absorption spectra of these subporphyrins show red-shifted bands, reflecting the expanded electronic network of the macrocycles.

2.12 *meso*-Alkenylidene-Substituted Subporphyrins. Oxocyclohexadienylidene-substituted subporphyrin **63**, which was prepared from *meso*-(3,5-di-*tert*-butyl-4-hydroxyphenyl)-substituted subporphyrin **62** by MnO_2 oxidation, exhibited quite different electronic and structural properties from typical subporphyrins. Deprotonation of **63** proceeded smoothly to provide the anionic species **64** (Figure 19).[161] In the crystal structure of **64-OH**, all *meso*-substituents exhibit distinct structural distortions resulting from nontrivial contribution of a quinonoidal form. The C–O bond lengths (1.23, 1.24, and 1.26 Å) are in the range of a quinone C–O double bond, and the C_{meso}–C_{ipso} bonds (1.38, 1.40, and 1.40 Å) show double bond character. The dihedral angles are all small (0.88, 4.98, and 6.68°). These structural features give rise to severe bending of all of the pyrrole units to avoid the steric congestion, causing a large bowl depth (1.56 Å). As a whole, the subporphyrin **64-OH** has a planar extended structure with almost C_3 symmetry.

2.13 Supramolecular Assembly. Axially coordinated monoanionic ligand on the central B(III) atom of subporphyrin is quantitatively and reversibly replaced by other ligands under suitable conditions. This property was used for the construction of supramolecular assembly. Namely, complementary face-to-face dimer formation from subporphyrin bearing a 2-carboxyphenyl group was explored.[162]

By means of Sonogashira coupling followed by Pd-catalyzed reduction of the alkynyl group, 2-carboxystyryl-substituted subporphyrin **65** was prepared in ca. 20% overall yield from 4-bromophenyl-substituted subporphyrin **9**. Reflux of a 200 μM toluene solution of **65** with continuous removal of methanol with a Dean–Stark trap led to the formation of dimer **66** (Scheme 9). Prolonged refluxing of this reaction mixture for 12 h resulted in the complete formation of **66**.[162] X-ray diffraction analysis revealed that the dimer **66** takes a complementary coordinated face-to-face dimer with C_2-sym-

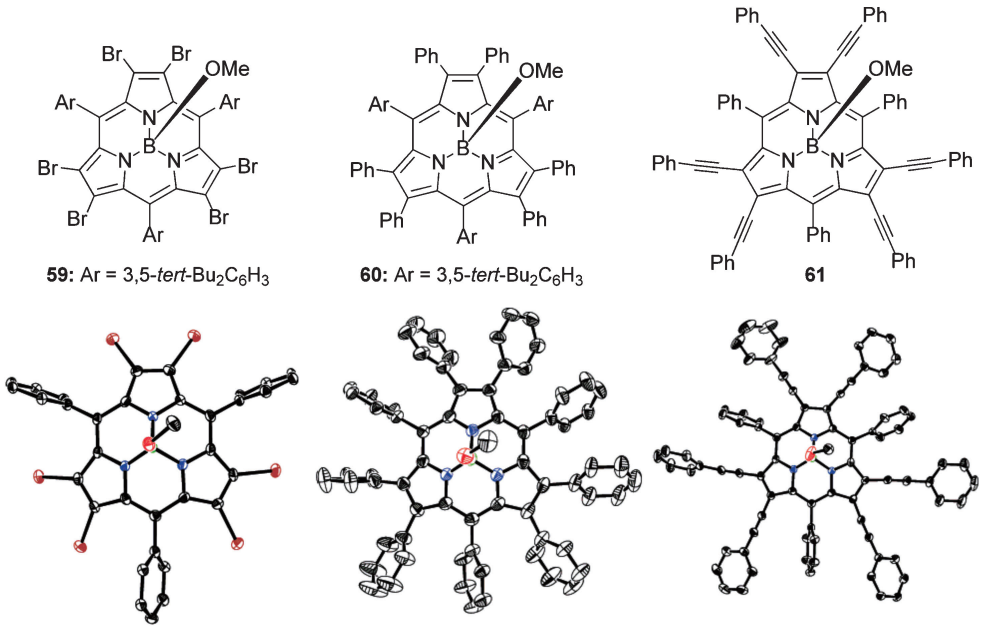

Figure 18. Crystal structures of peripherally hexasubstituted subporphyrins (*tert*-butyl groups are omitted.).

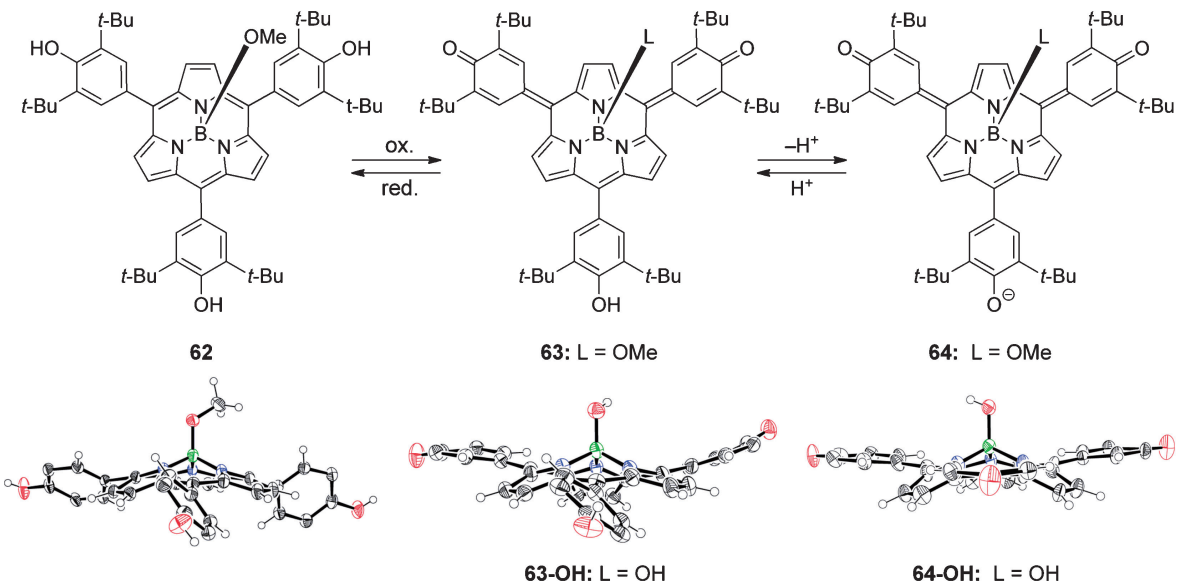

Figure 19. Oxocyclohexadienylidene-substituted subporphyrins and the crystal structures of **62**, **63-OH**, and **64-OH**.

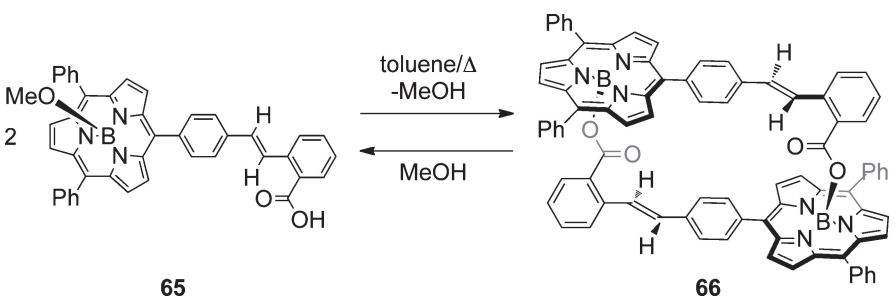

Scheme 9. Interconversion between **65** and **66**.

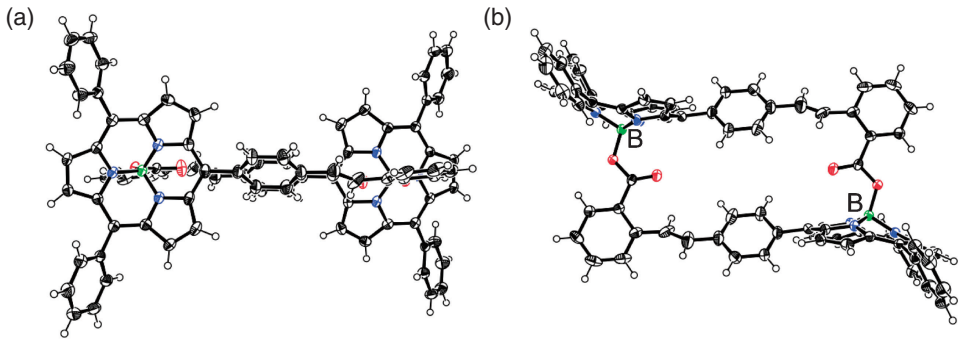

Figure 20. Crystal structure of **66**; (a) top view, (b) side view.

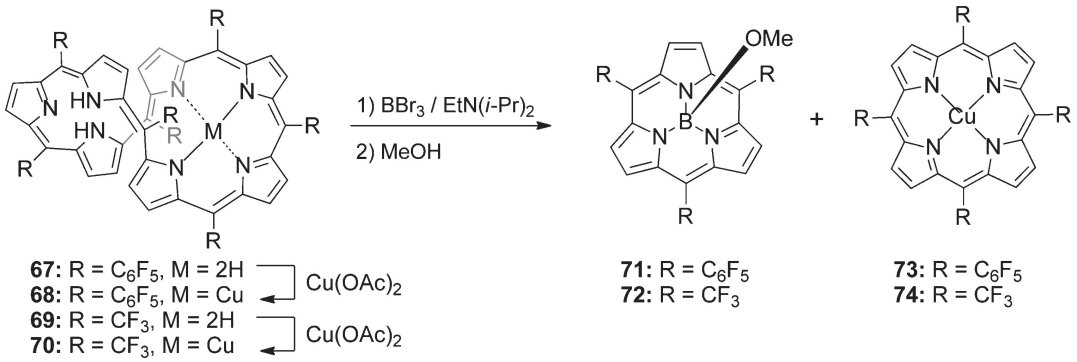

Scheme 10. Splitting reactions.

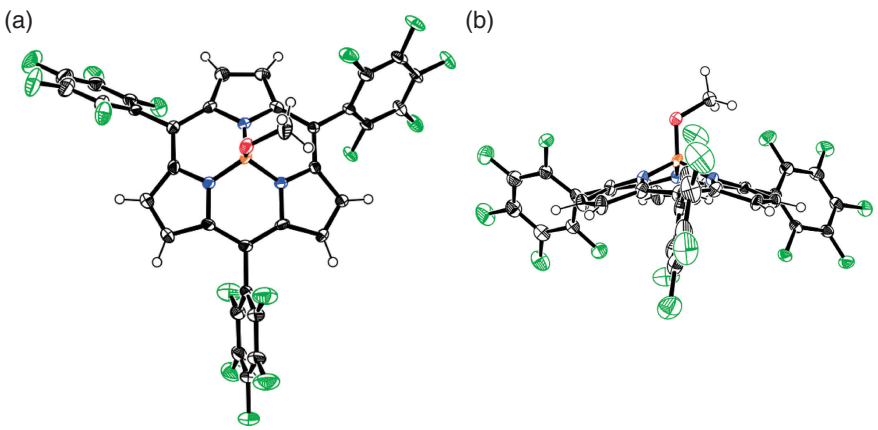

Figure 21. Crystal structure of **71**; (a) top view, (b) side view.

metry. The inner square cavity is roughly defined with ca. 8 Å length and ca. 6 Å height (Figure 20). Interestingly, the dimer **66** is stable toward hydrolysis in aqueous solution, although an axially benzoyloxy coordinated subporphyrin monomer is quite susceptible to hydrolysis in the presence of water. On the other hand, treatment of **66** with a mixture of CH_2Cl_2 and methanol at 40 °C resulted in quantitative recovery of monomer **65** (Scheme 9). Thermal and moisture stable assembly utilizing B(III)-coordination will be useful for the organization of large discrete constructs.

2.14 Formation of Subporphyrins from Metalation-Induced Splitting Reactions. *meso*-Pentafluorophenyl-substituted [32]heptaphyrin **67** was synthesized by means of [3 + 4] MacDonald-type condensation of tripyrrane dicarbinol and tetrapyrrane.[163] Metalation of **67** with $Cu(OAc)_2$ resulted in quantitative formation of mono-Cu(II) complex **68**. In the solid state, **68** shows a twisted structure consisting of porphyrin-like unit and tripyrrolic segment with a pseudo C_2-symmetry, where copper ion is bound to the porphyrinic segment in a square-planar fashion.[91] In order to explore the possibility of ring-splitting reaction of heptaphyrins, B(III) complexation into the remaining tripyrrolic segments of **68** was attempted by treatment with boron trihalide under various conditions. Upon treatment with 100 equiv of BBr_3 in the presence of $EtN(i\text{-}Pr)_2$ at room temperature, the complex **68** disappeared readily to give a complicated mixture that included *meso*-pentafluorophenyl-substituted subporphyrin **71** and Cu(II) porphyrin **73** (Scheme 10).[66,91,164] The optimized yields were 36 and 13% yields for **71** and **73** respectively. The structure of subporphyrin **71** was determined by X-ray diffraction analysis to be a bowl shape (Figure 21). Three pentafluorophenyl groups are tilted by 61–79° relative to the subporphyrin framework and these tilting

angles are higher than those of subporphyrins with *ortho*-unsubstituted *meso*-aryl groups. ^{19}F NMR spectroscopy revealed hindered rotation of the *meso*-pentafluorophenyl groups in **71** even at 140 °C in solution. Since subporphyrin **72** cannot be synthesized by our Alder-type protocol from 1-(tri-1-pyrrolylboryl)pyridine **6**, this extrusion reaction is synthetically important. Using the same strategy, *meso*-trifluoromethyl-substituted subporphyrin **72** was obtained from *meso*-trifluoromethyl-substituted heptaphyrin **70** in 12% yield along with *meso*-trifluoromethyl-substituted Cu(II) porphyrin **74**.[92]

3. Summary

In this account, our efforts in the chemistry of *meso–meso*-linked porphyrin arrays, *meso*-aryl expanded porphyrins, and iridium-catalyzed β-selective direct borylation are briefly reviewed. A focus is placed on the chemistry of subporphyrins. Since the first synthesis of tribenzosubporphines in 2006, *meso*-aryl-substituted subporphyrins, *meso*-heteroaryl-substituted subporphyrins, *meso*-alkyl-substituted subporphyrins, capped subporphyrins, subchlorins, subbacteriochlorins, and oxocyclohexadienylidene-substituted subporphyrin have been synthesized and characterized. Porphyrin–subporphyrin hybrids, dipyrromethene–subporphyrin hybrids, and supramolecular assemblies of subporphyrins have been also explored. The peripheral modification methods such as bromination, Suzuki–Miyaura coupling, and Stille coupling have been developed. In addition, the B(III) and Cu(II) combined metalation-induced splitting of heptaphyrins has been shown to provide tris(pentafluorophenyl)-substituted and tris(trifluoromethyl)-substituted subporphyrins that are difficult to make by the standard method. Subporphyrins are unique and interesting chromophores, exhibiting a bowl-shaped 14π-electronic aromatic circuit, porphyrin-like intense absorption, intense green fluorescence, and large substituent effects. The electronic systems of subporphyrins are quite flexible and thus tunable by *meso*-aryl substituents. Despite these progresses, the chemistry of subporphyrins is still in the infant stage and improvement in the synthetic yields of subporphyrins is obviously required for future developments. As described above, all the subporphyrins contain boron(III) ion in their cavity. The synthesis and characterization of free base subporphyrins will be an interesting next target. Finally it is noted that triphyrins(2.1.1), other ring-contracted porphyrinoids, have been recently prepared in unexpected and rational routes as a new promising macrocycle, which show planar structures and strong aromaticity due to 14π-electronic networks.[165] Although the chemistry of these ring-contracted porphyrinoids has advanced rapidly in recent years, it is clear that much more work remains to be done, particularly in fields of material science and molecular devices.

This work was partly supported by Grants-in-Aid No. 22245006 (A) and No. 20108006 "pi-Space" from MEXT. T.T. and E.T. thank the JSPS Research Fellowships for Young Scientists. We thank Prof. Dongho Kim of Yonsei University and his group members for the optical measurements and theoretical studies. Finally, special thanks are given to those listed as the coauthors in our papers cited here, particularly to Dr. Y. Inokuma and S. Hayashi for their outstanding contribution to these results.

References

1 a) K. Maruyama, A. Osuka, *Pure Appl. Chem.* **1990**, *62*, 1511. b) K. Maruyama, A. Osuka, N. Mataga, *Pure Appl. Chem.* **1994**, *66*, 867. c) A. Osuka, N. Mataga, T. Okada, *Pure Appl. Chem.* **1997**, *69*, 797.

2 a) A. Osuka, K. Maruyama, *J. Am. Chem. Soc.* **1988**, *110*, 4454. b) A. Osuka, K. Maruyama, I. Yamazaki, N. Tamai, *Chem. Phys. Lett.* **1990**, *165*, 392. c) T. Nagata, A. Osuka, K. Maruyama, *J. Am. Chem. Soc.* **1990**, *112*, 3054. d) A. Osuka, K. Maruyama, N. Mataga, T. Asahi, I. Yamazaki, N. Tamai, *J. Am. Chem. Soc.* **1990**, *112*, 4958. e) A. Osuka, S. Nakajima, T. Nagata, K. Maruyama, K. Toriumi, *Angew. Chem., Int. Ed. Engl.* **1991**, *30*, 582.

3 a) A. Osuka, S. Nakajima, K. Maruyama, N. Mataga, T. Asahi, I. Yamazaki, Y. Nishimura, T. Ohno, K. Nozaki, *J. Am. Chem. Soc.* **1993**, *115*, 4577. b) M. Ohkohchi, A. Takahashi, N. Mataga, T. Okada, A. Osuka, H. Yamada, K. Maruyama, *J. Am. Chem. Soc.* **1993**, *115*, 12137. c) A. Osuka, H. Yamada, K. Maruyama, N. Mataga, T. Asahi, M. Ohkouchi, T. Okada, I. Yamazaki, Y. Nishimura, *J. Am. Chem. Soc.* **1993**, *115*, 9439. d) A. Osuka, S. Nakajima, T. Okada, S. Taniguchi, K. Nozaki, T. Ohno, I. Yamazaki, Y. Nishimura, N. Mataga, *Angew. Chem., Int. Ed. Engl.* **1996**, *35*, 92. e) A. Osuka, S. Marumo, N. Mataga, S. Taniguchi, T. Okada, I. Yamazaki, Y. Nishimura, T. Ohno, K. Nozaki, *J. Am. Chem. Soc.* **1996**, *118*, 155.

4 A. Osuka, H. Shimidzu, *Angew. Chem., Int. Ed. Engl.* **1997**, *36*, 135.

5 J. E. Baldwin, M. J. Crossley, J. DeBernardis, *Tetrahedron* **1982**, *38*, 685.

6 a) N. Aratani, A. Osuka, Y. H. Kim, D. H. Jeong, D. Kim, *Angew. Chem., Int. Ed.* **2000**, *39*, 1458. b) N. Aratani, A. Takagi, Y. Yanagawa, T. Matsumoto, T. Kawai, Z. S. Yoon, D. Kim, A. Osuka, *Chem.—Eur. J.* **2005**, *11*, 3389.

7 A. Nakano, A. Osuka, I. Yamazaki, T. Yamazaki, Y. Nishimura, *Angew. Chem., Int. Ed.* **1998**, *37*, 3023.

8 A. Nakano, T. Yamazaki, Y. Nishimura, I. Yamazaki, A. Osuka, *Chem.—Eur. J.* **2000**, *6*, 3254.

9 A. Nakano, A. Osuka, T. Yamazaki, Y. Nishimura, S. Akimoto, I. Yamazaki, A. Itaya, M. Murakami, H. Miyasaka, *Chem.—Eur. J.* **2001**, *7*, 3134.

10 N. Yoshida, A. Osuka, *Org. Lett.* **2000**, *2*, 2963.

11 N. Yoshida, T. Ishizuka, A. Osuka, D. H. Jeong, H. S. Cho, D. Kim, Y. Matsuzaki, A. Nogami, K. Tanaka, *Chem.—Eur. J.* **2003**, *9*, 58.

12 X. Peng, N. Aratani, A. Takagi, T. Matsumoto, T. Kawai, I.-W. Hwang, T. K. Ahn, D. Kim, A. Osuka, *J. Am. Chem. Soc.* **2004**, *126*, 4468.

13 T. Hori, N. Aratani, A. Takagi, T. Matsumoto, T. Kawai, M.-C. Yoon, Z. S. Yoon, S. Cho, D. Kim, A. Osuka, *Chem.—Eur. J.* **2006**, *12*, 1319.

14 T. Hori, X. Peng, N. Aratani, A. Takagi, T. Matsumoto, T. Kawai, Z. S. Yoon, M.-C. Yoon, J. Yang, D. Kim, A. Osuka, *Chem.—Eur. J.* **2008**, *14*, 582.

15 C. Ikeda, Z. S. Yoon, M. Park, H. Inoue, D. Kim, A. Osuka, *J. Am. Chem. Soc.* **2005**, *127*, 534.

16 Y. Nakamura, I.-W. Hwang, N. Aratani, T. K. Ahn, D. M. Ko, A. Takagi, T. Kawai, T. Matsumoto, D. Kim, A. Osuka, *J. Am. Chem. Soc.* **2005**, *127*, 236.

17 A. Tsuda, T. Nakamura, S. Sakamoto, K. Yamaguchi, A. Osuka, *Angew. Chem., Int. Ed.* **2002**, *41*, 2817.

18 I.-W. Hwang, T. Kamada, T. K. Ahn, D. M. Ko, T. Nakamura, A. Tsuda, A. Osuka, D. Kim, *J. Am. Chem. Soc.* **2004**,

126, 16187.
19 T. Kamada, N. Aratani, T. Ikeda, N. Shibata, Y. Higuchi, A. Wakamiya, S. Yamaguchi, K. S. Kim, Z. S. Yoon, D. Kim, A. Osuka, *J. Am. Chem. Soc.* **2006**, *128*, 7670.
20 C. Maeda, T. Kamada, N. Aratani, T. Sasamori, N. Tokitoh, A. Osuka, *Chem.—Eur. J.* **2009**, *15*, 9681.
21 A. Tsuda, H. Furuta, A. Osuka, *Angew. Chem., Int. Ed.* **2000**, *39*, 2549.
22 A. Tsuda, H. Furuta, A. Osuka, *J. Am. Chem. Soc.* **2001**, *123*, 10304.
23 A. Tsuda, A. Osuka, *Science* **2001**, *293*, 79.
24 T. Ikeda, A. Tsuda, N. Aratani, A. Osuka, *Chem. Lett.* **2006**, *35*, 946.
25 T. Ikeda, J. M. Lintuluoto, N. Aratani, Z. S. Yoon, D. Kim, A. Osuka, *Eur. J. Org. Chem.* **2006**, 3193.
26 T. Ikeda, N. Aratani, A. Osuka, *Chem.—Asian J.* **2009**, *4*, 1248.
27 a) Y. Nakamura, N. Aratani, H. Shinokubo, A. Takagi, T. Kawai, T. Matsumoto, Z. S. Yoon, D. Y. Kim, T. K. Ahn, D. Kim, A. Muranaka, N. Kobayashi, A. Osuka, *J. Am. Chem. Soc.* **2006**, *128*, 4119. b) Y. Nakamura, N. Aratani, A. Osuka, *Chem.—Asian J.* **2007**, *2*, 860. c) Y. Nakamura, N. Aratani, K. Furukawa, A. Osuka, *Tetrahedron* **2008**, *64*, 11433.
28 Y. Nakamura, S. Y. Jang, T. Tanaka, N. Aratani, J. M. Lim, K. S. Kim, D. Kim, A. Osuka, *Chem.—Eur. J.* **2008**, *14*, 8279.
29 a) T. Tanaka, Y. Nakamura, A. Osuka, *Chem.—Eur. J.* **2008**, *14*, 204. b) T. Tanaka, Y. Nakamura, N. Aratani, A. Osuka, *Tetrahedron Lett.* **2008**, *49*, 3308.
30 D. Bonifazi, M. Scholl, F. Song, L. Echegoyen, G. Accorsi, N. Armaroli, F. Diederich, *Angew. Chem., Int. Ed.* **2003**, *42*, 4966.
31 D. Bonifazi, H. Spillmann, A. Kiebele, M. de Wild, P. Seiler, F. Cheng, H.-J. Güntherodt, T. Jung, F. Diederich, *Angew. Chem., Int. Ed.* **2004**, *43*, 4759.
32 L.-A. Fendt, H. Fang, M. E. Plonska-Brzezinska, S. Zhang, F. Cheng, C. Braun, L. Echegoyen, F. Diederich, *Eur. J. Org. Chem.* **2007**, 4659.
33 H. Sato, K. Tashiro, H. Shinmori, A. Osuka, T. Aida, *Chem. Commun.* **2005**, 2324.
34 H. Sato, K. Tashiro, H. Shinmori, A. Osuka, Y. Murata, K. Komatsu, T. Aida, *J. Am. Chem. Soc.* **2005**, *127*, 13086.
35 a) T. Sakurai, K. Shi, H. Sato, K. Tashiro, A. Osuka, A. Saeki, S. Seki, S. Tagawa, S. Sasaki, H. Masunaga, K. Osaka, M. Takata, T. Aida, *J. Am. Chem. Soc.* **2008**, *130*, 13812. b) T. Sakurai, K. Tashiro, Y. Honsho, A. Saeki, S. Seki, A. Osuka, A. Muranaka, M. Uchiyama, J. Kim, S. Ha, K. Kato, M. Takata, T. Aida, *J. Am. Chem. Soc.* **2011**, *133*, 6537.
36 I. M. Blake, A. Krivokapic, M. Katterle, H. L. Anderson, *Chem. Commun.* **2002**, 1662.
37 N. Aratani, A. Osuka, *Macromol. Rapid Commun.* **2001**, *22*, 725.
38 N. Aratani, A. Osuka, *Bull. Chem. Soc. Jpn.* **2001**, *74*, 1361.
39 N. Aratani, A. Tsuda, A. Osuka, *Synlett* **2001**, 1663.
40 N. Aratani, A. Osuka, H. S. Cho, D. Kim, *J. Photochem. Photobiol., C* **2002**, *3*, 25.
41 D. Kim, A. Osuka, *J. Phys. Chem. A* **2003**, *107*, 8791.
42 N. Aratani, A. Osuka, *Chem. Rec.* **2003**, *3*, 225.
43 D. Kim, A. Osuka, *Acc. Chem. Res.* **2004**, *37*, 735.
44 N. Aratani, D. Kim, A. Osuka, *Chem.—Asian J.* **2009**, *4*, 1172.
45 N. Aratani, D. Kim, A. Osuka, *Acc. Chem. Res.* **2009**, *42*, 1922.
46 A. Jasat, D. Dolphin, *Chem. Rev.* **1997**, *97*, 2267.
47 J. L. Sessler, S. J. Weghorn, *Expanded, Contracted & Isomeric Porphyrins* in *Tetrahedron Organic Chemistry Series*, Pergamon Press, **1997**, Vol. 15.
48 J. L. Sessler, D. Seidel, *Angew. Chem., Int. Ed.* **2003**, *42*, 5134.
49 T. D. Lash, *Angew. Chem., Int. Ed.* **2000**, *39*, 1763.
50 T. K. Chandrashekar, S. Venkatraman, *Acc. Chem. Res.* **2003**, *36*, 676.
51 R. Misra, T. K. Chandrashekar, *Acc. Chem. Res.* **2008**, *41*, 265.
52 S. Shimizu, A. Osuka, *Eur. J. Inorg. Chem.* **2006**, 1319.
53 A. Osuka, S. Saito, *Chem. Commun.* **2011**, *47*, 4330.
54 M. Stępień, N. Sprutta, L. Latos-Grażyński, *Angew. Chem., Int. Ed.* **2011**, *50*, 4288.
55 S. Saito, A. Osuka, *Angew. Chem., Int. Ed.* **2011**, *50*, 4342.
56 M. G. P. M. S. Neves, R. M. Martins, A. C. Tomé, A. J. D. Silvestre, A. M. S. Silva, V. Félix, J. A. S. Cavaleiro, M. G. B. Drew, *Chem. Commun.* **1999**, 385.
57 J. S. Lindsey, I. C. Schreiman, H. C. Hsu, P. C. Kearney, A. M. Marguerettaz, *J. Org. Chem.* **1987**, *52*, 827.
58 J.-Y. Shin, H. Furuta, A. Osuka, *Angew. Chem., Int. Ed.* **2001**, *40*, 619.
59 J.-Y. Shin, H. Furuta, K. Yoza, S. Igarashi, A. Osuka, *J. Am. Chem. Soc.* **2001**, *123*, 7190.
60 R. Taniguchi, S. Shimizu, M. Suzuki, J.-Y. Shin, H. Furuta, A. Osuka, *Tetrahedron Lett.* **2003**, *44*, 2505.
61 Y. Kamimura, S. Shimizu, A. Osuka, *Chem.—Eur. J.* **2007**, *13*, 1620.
62 Y. Tanaka, J.-Y. Shin, A. Osuka, *Eur. J. Org. Chem.* **2008**, 1341.
63 S. Shimizu, V. G. Anand, R. Taniguchi, K. Furukawa, T. Kato, T. Yokoyama, A. Osuka, *J. Am. Chem. Soc.* **2004**, *126*, 12280.
64 S. Mori, A. Osuka, *J. Am. Chem. Soc.* **2005**, *127*, 8030.
65 S. Mori, K. S. Kim, Z. S. Yoon, S. B. Noh, D. Kim, A. Osuka, *J. Am. Chem. Soc.* **2007**, *129*, 11344.
66 S. Saito, K. Furukawa, A. Osuka, *Angew. Chem., Int. Ed.* **2009**, *48*, 8086.
67 S. Mori, S. Shimizu, J.-Y. Shin, A. Osuka, *Inorg. Chem.* **2007**, *46*, 4374.
68 a) S. Mori, A. Osuka, *Inorg. Chem.* **2008**, *47*, 3937. b) H. Rath, N. Aratani, J. M. Lim, J. S. Lee, D. Kim, H. Shinokubo, A. Osuka, *Chem. Commun.* **2009**, 3762.
69 T. Koide, G. Kashiwazaki, K. Furukawa, A. Osuka, *Inorg. Chem.* **2009**, *48*, 4595.
70 T. Koide, G. Kashiwazaki, M. Suzuki, K. Furukawa, M.-C. Yoon, S. Cho, D. Kim, A. Osuka, *Angew. Chem., Int. Ed.* **2008**, *47*, 9661.
71 Y. Tanaka, S. Saito, S. Mori, N. Aratani, H. Shinokubo, N. Shibata, Y. Higuchi, Z. S. Yoon, K. S. Kim, S. B. Noh, J. K. Park, D. Kim, A. Osuka, *Angew. Chem., Int. Ed.* **2008**, *47*, 681.
72 J. K. Park, Z. S. Yoon, M.-C. Yoon, K. S. Kim, S. Mori, J.-Y. Shin, A. Osuka, D. Kim, *J. Am. Chem. Soc.* **2008**, *130*, 1824.
73 J. Sankar, S. Mori, S. Saito, H. Rath, M. Suzuki, Y. Inokuma, H. Shinokubo, K. S. Kim, Z. S. Yoon, J.-Y. Shin, J. M. Lim, Y. Matsuzaki, O. Matsushita, A. Muranaka, N. Kobayashi, D. Kim, A. Osuka, *J. Am. Chem. Soc.* **2008**, *130*, 13568.
74 S. Tokuji, J.-Y. Shin, K. S. Kim, J. M. Lim, K. Youfu, S. Saito, D. Kim, A. Osuka, *J. Am. Chem. Soc.* **2009**, *131*, 7240.
75 M. Inoue, K. S. Kim, M. Suzuki, J. M. Lim, J.-Y. Shin, D. Kim, A. Osuka, *Angew. Chem., Int. Ed.* **2009**, *48*, 6687.

76 a) T. Koide, K. Youfu, S. Saito, A. Osuka, *Chem. Commun.* **2009**, 6047. b) T. Koide, A. Osuka, *Bull. Chem. Soc. Jpn.* **2010**, *83*, 877.
77 J. M. Lim, J.-Y. Shin, Y. Tanaka, S. Saito, A. Osuka, D. Kim, *J. Am. Chem. Soc.* **2010**, *132*, 3105.
78 T. Higashino, M. Inoue, A. Osuka, *J. Org. Chem.* **2010**, *75*, 7958.
79 M. Inoue, A. Osuka, *Angew. Chem., Int. Ed.* **2010**, *49*, 9488.
80 T. Tanaka, T. Sugita, S. Tokuji, S. Saito, A. Osuka, *Angew. Chem., Int. Ed.* **2010**, *49*, 6619.
81 T. Higashino, J. M. Lim, T. Miura, S. Saito, J.-Y. Shin, D. Kim, A. Osuka, *Angew. Chem., Int. Ed.* **2010**, *49*, 4950.
82 The first example of Möbius antiaromatic species was reported for a protonated Pd(II) complex of vacataporphyrin; E. Pacholska-Dudziak, J. Skonieczny, M. Pawlicki, L. Szterenberg, Z. Ciunik, L. Latos-Grażyński, *J. Am. Chem. Soc.* **2008**, *130*, 6182.
83 H. Rath, S. Tokuji, N. Aratani, K. Furukawa, J. M. Lim, D. Kim, H. Shinokubo, A. Osuka, *Angew. Chem., Int. Ed.* **2010**, *49*, 1489.
84 T. Koide, K. Furukawa, H. Shinokubo, J.-Y. Shin, K. S. Kim, D. Kim, A. Osuka, *J. Am. Chem. Soc.* **2010**, *132*, 7246.
85 M. Suzuki, A. Osuka, *Angew. Chem., Int. Ed.* **2007**, *46*, 5171.
86 M. Suzuki, A. Osuka, *J. Am. Chem. Soc.* **2007**, *129*, 464.
87 L. Latos-Grażyński, *Angew. Chem., Int. Ed.* **2004**, *43*, 5124.
88 M. O. Senge, N. N. Sergeeva, *Angew. Chem., Int. Ed.* **2006**, *45*, 7492.
89 Y. Tanaka, W. Hoshino, S. Shimizu, K. Youfu, N. Aratani, N. Maruyama, S. Fujita, A. Osuka, *J. Am. Chem. Soc.* **2004**, *126*, 3046.
90 Y. Tanaka, H. Shinokubo, Y. Yoshimura, A. Osuka, *Chem.—Eur. J.* **2009**, *15*, 5674.
91 S. Saito, K. S. Kim, Z. S. Yoon, D. Kim, A. Osuka, *Angew. Chem., Int. Ed.* **2007**, *46*, 5591.
92 R. Sakamoto, S. Saito, S. Shimizu, Y. Inokuma, N. Aratani, A. Osuka, *Chem. Lett.* **2010**, *39*, 439.
93 K. Moriya, S. Saito, A. Osuka, *Angew. Chem., Int. Ed.* **2010**, *49*, 4297.
94 T. Yoneda, S. Saito, H. Yorimitsu, A. Osuka, *Angew. Chem., Int. Ed.* **2011**, *50*, 3475.
95 Y. Tanaka, H. Mori, T. Koide, H. Yorimitsu, A. Osuka, *Chem.—Eur. J.*, submitted.
96 Z. S. Yoon, A. Osuka, D. Kim, *Nat. Chem.* **2009**, *1*, 113.
97 M. O. Senge, *Chem. Commun.* **2011**, *47*, 1943.
98 M. O. Senge, Y. M. Shaker, M. Pintea, C. Ryppa, S. S. Hatscher, A. Ryan, Y. Sergeeva, *Eur. J. Org. Chem.* **2010**, 237.
99 T. Ren, *Chem. Rev.* **2008**, *108*, 4185.
100 B. M. J. M. Suijkerbuijk, R. J. M. Klein Gebbink, *Angew. Chem., Int. Ed.* **2008**, *47*, 7396.
101 F. Atefi, D. P. Arnold, *J. Porphyrins Phthalocyanines* **2008**, *12*, 801.
102 N. N. Sergeeva, M. O. Senge, A. Ryan, in *Handbook of Porphyrin Science: With Applications to Chemistry, Physics, Materials Science, Engineering, Biology and Medicine*, ed. by K. M. Kadish, K. M. Smith, R. Guilard, World Scientific Publishing, **2010**, Vol. 3, Chap. 13.
103 W. M. Sharman, J. E. Van Lier, *J. Porphyrins Phthalocyanines* **2000**, *4*, 441.
104 R. W. Wagner, J. S. Lindsey, *J. Am. Chem. Soc.* **1994**, *116*, 9759.
105 J. Li, A. Ambroise, S. I. Yang, J. R. Diers, J. Seth, C. R. Wack, D. F. Bocian, D. Holten, J. S. Lindsey, *J. Am. Chem. Soc.* **1999**, *121*, 8927.
106 V. S. Lin, S. G. DiMagno, M. J. Therien, *Science* **1994**, *264*, 1105.
107 S. G. DiMagno, V. S. Y. Lin, M. J. Therien, *J. Am. Chem. Soc.* **1993**, *115*, 2513.
108 A. G. Hyslop, M. A. Kellett, P. M. Iovine, M. J. Therien, *J. Am. Chem. Soc.* **1998**, *120*, 12676.
109 N. Aratani, A. Osuka, *Org. Lett.* **2001**, *3*, 4213.
110 J. T. Fletcher, M. J. Therien, *J. Am. Chem. Soc.* **2000**, *122*, 12393.
111 J. T. Fletcher, M. J. Therien, *J. Am. Chem. Soc.* **2002**, *124*, 4298.
112 M. Takase, R. Ismael, R. Murakami, M. Ikeda, D. Kim, H. Shinmori, H. Furuta, A. Osuka, *Tetrahedron Lett.* **2002**, *43*, 5157.
113 H. S. Cho, H. Rhee, J. K. Song, C.-K. Min, M. Takase, N. Aratani, S. Cho, A. Osuka, T. Joo, D. Kim, *J. Am. Chem. Soc.* **2003**, *125*, 5849.
114 G. Kodis, Y. Terazono, P. A. Liddell, J. Andréasson, V. Garg, M. Hambourger, T. A. Moore, A. L. Moore, D. Gust, *J. Am. Chem. Soc.* **2006**, *128*, 1818.
115 H. Hata, H. Shinokubo, A. Osuka, *J. Am. Chem. Soc.* **2005**, *127*, 8264.
116 T. Ishiyama, J. Takagi, K. Ishida, N. Miyaura, N. R. Anastasi, J. F. Hartwig, *J. Am. Chem. Soc.* **2002**, *124*, 390.
117 T. Ishiyama, N. Miyaura, *J. Organomet. Chem.* **2003**, *680*, 3.
118 H. Baba, J. Chen, H. Shinokubo, A. Osuka, *Chem.—Eur. J.* **2008**, *14*, 4256.
119 J. Chen, N. Aratani, H. Shinokubo, A. Osuka, *Chem.—Asian J.* **2009**, *4*, 1126.
120 H. Hata, S. Yamaguchi, G. Mori, S. Nakazono, T. Katoh, K. Takatsu, S. Hiroto, H. Shinokubo, A. Osuka, *Chem.—Asian J.* **2007**, *2*, 849.
121 J. Song, N. Aratani, P. Kim, D. Kim, H. Shinokubo, A. Osuka, *Angew. Chem., Int. Ed.* **2010**, *49*, 3617.
122 I. Hisaki, S. Hiroto, K. S. Kim, S. B. Noh, D. Kim, H. Shinokubo, A. Osuka, *Angew. Chem., Int. Ed.* **2007**, *46*, 5125.
123 J. Song, S. Y. Jang, S. Yamagichi, J. Sankar, S. Hiroto, N. Aratani, J.-Y. Shin, S. Easwaramoorthi, K. S. Kim, D. Kim, H. Shinokubo, A. Osuka, *Angew. Chem., Int. Ed.* **2008**, *47*, 6004.
124 J. Song, P. Kim, N. Aratani, D. Kim, H. Shinokubo, A. Osuka, *Chem.—Eur. J.* **2010**, *16*, 3009.
125 J. Song, N. Aratani, H. Shinokubo, A. Osuka, *Chem. Sci.* **2011**, *2*, 748.
126 S. Hiroto, I. Hisaki, H. Shinokubo, A. Osuka, *Angew. Chem., Int. Ed.* **2005**, *44*, 6763.
127 S. Hiroto, K. Furukawa, H. Shinokubo, A. Osuka, *J. Am. Chem. Soc.* **2006**, *128*, 12380.
128 S. Hiroto, N. Aratani, N. Shibata, Y. Higuchi, T. Sasamori, N. Tokitoh, H. Shinokubo, A. Osuka, *Angew. Chem., Int. Ed.* **2009**, *48*, 2388.
129 S. Hiroto, I. Hisaki, H. Shinokubo, A. Osuka, *J. Am. Chem. Soc.* **2008**, *130*, 16172.
130 S. Yamaguchi, T. Katoh, H. Shinokubo, A. Osuka, *J. Am. Chem. Soc.* **2007**, *129*, 6392.
131 S. Yamaguchi, T. Katoh, H. Shinokubo, A. Osuka, *J. Am. Chem. Soc.* **2008**, *130*, 14440.
132 S. Yamaguchi, H. Shinokubo, A. Osuka, *J. Am. Chem. Soc.* **2010**, *132*, 9992.
133 J. Song, N. Aratani, J. H. Heo, D. Kim, H. Shinokubo, A. Osuka, *J. Am. Chem. Soc.* **2010**, *132*, 11868.

134 J. Song, N. Aratani, H. Shinokubo, A. Osuka, *J. Am. Chem. Soc.* **2010**, *132*, 16356.
135 H. Shinokubo, A. Osuka, *Chem. Commun.* **2009**, 1011.
136 Y. Inokuma, A. Osuka, *Dalton Trans.* **2008**, 2517.
137 Y. Inokuma, J. H. Kwon, T. K. Ahn, M.-C. Yoo, D. Kim, A. Osuka, *Angew. Chem., Int. Ed.* **2006**, *45*, 961.
138 A. Meller, A. Ossko, *Monatsh. Chem.* **1972**, *103*, 150.
139 a) C. G. Claessens, D. González-Rodríguez, T. Torres, *Chem. Rev.* **2002**, *102*, 835. b) G. de la Torre, P. Vázquez, F. Agulló-López, T. Torres, *Chem. Rev.* **2004**, *104*, 3723.
140 T. Torres, *Angew. Chem., Int. Ed.* **2006**, *45*, 2834.
141 a) M. S. Rodríguez-Morgade, S. Esperanza, T. Torres, J. Barberá, *Chem.—Eur. J.* **2005**, *11*, 354. b) J. R. Stork, J. J. Brewer, T. Fukuda, J. P. Fitzgerald, G. T. Yee, A. Y. Nazarenko, N. Kobayashi, W. S. Durfee, *Inorg. Chem.* **2006**, *45*, 6148. c) M. S. Rodríguez-Morgade, C. G. Claessens, A. Medina, D. González-Rodríguez, E. Gutiérrez-Puebla, A. Monge, I. Alkorta, J. Elguero, T. Torres, *Chem.—Eur. J.* **2008**, *14*, 1342.
142 L. Edwards, M. Gouterman, C. B. Rose, *J. Am. Chem. Soc.* **1976**, *98*, 7638.
143 R. Myśliborski, L. Latos-Grażyński, L. Szterenberg, T. Lis, *Angew. Chem., Int. Ed.* **2006**, *45*, 3670.
144 a) A. Krivokapic, A. R. Cowley, H. L. Anderson, *J. Org. Chem.* **2003**, *68*, 1089. b) A. Berlicka, L. Latos-Grażyński, T. Lis, *Angew. Chem., Int. Ed.* **2005**, *44*, 5288.
145 a) N. Kobayashi, Y. Takeuchi, A. Matsuda, *Angew. Chem., Int. Ed.* **2007**, *46*, 758. b) Y. Takeuchi, A. Matsuda, N. Kobayashi, *J. Am. Chem. Soc.* **2007**, *129*, 8271.
146 a) Y. Inokuma, Z. S. Yoon, D. Kim, A. Osuka, *J. Am. Chem. Soc.* **2007**, *129*, 4747. b) Y. Inokuma, S. Easwaramoorthi, S. Y. Jang, K. S. Kim, D. Kim, A. Osuka, *Angew. Chem., Int. Ed.* **2008**, *47*, 4840.
147 B. H. Yang, S. L. Buchwald, *J. Organomet. Chem.* **1999**, *576*, 125.
148 Y. Inokuma, S. Easwaramoorthi, Z. S. Yoon, D. Kim, A. Osuka, *J. Am. Chem. Soc.* **2008**, *130*, 12234.
149 a) J. Lindsey, *J. Org. Chem.* **1980**, *45*, 5215. b) J. S. Lindsey, D. C. Mauzerall, *J. Am. Chem. Soc.* **1982**, *104*, 4498.
150 Y. Inokuma, A. Osuka, *Chem.—Eur. J.* **2009**, *15*, 6863.
151 Y. Inokuma, S. Hayashi, A. Osuka, *Chem. Lett.* **2009**, *38*, 206.
152 H. Sugimoto, M. Muto, T. Tanaka, A. Osuka, *Eur. J. Org. Chem.* **2011**, 71.
153 H. Sugimoto, T. Tanaka, A. Osuka, *Chem. Lett.* **2011**, *40*, 629.
154 S. Hayashi, Y. Inokuma, A. Osuka, *Org. Lett.* **2010**, *12*, 4148.
155 Y. Inokuma, A. Osuka, *Org. Lett.* **2008**, *10*, 5561.
156 S. Hayashi, Y. Inokuma, S. Easwaramoorthi, K. S. Kim, D. Kim, A. Osuka, *Angew. Chem., Int. Ed.* **2010**, *49*, 321.
157 E. Tsurumaki, S. Saito, K. S. Kim, J. M. Lim, Y. Inokuma, D. Kim, A. Osuka, *J. Am. Chem. Soc.* **2008**, *130*, 438.
158 A. D. Adler, F. R. Longo, J. D. Finarelli, J. Goldmacher, J. Assour, L. Korsakoff, *J. Org. Chem.* **1967**, *32*, 476.
159 S. Hayashi, E. Tsurumaki, Y. Inokuma, P. Kim, Y. M. Sung, D. Kim, A. Osuka, *J. Am. Chem. Soc.* **2011**, *133*, 4254.
160 E. Tsurumaki, Y. Inokuma, S. Easwaramoorthi, J. M. Lim, D. Kim, A. Osuka, *Chem.—Eur. J.* **2009**, *15*, 237.
161 S. Hayashi, J. Sung, Y. M. Sung, Y. Inokuma, D. Kim, A. Osuka, *Angew. Chem., Int. Ed.* **2011**, *50*, 3253.
162 Y. Inokuma, A. Osuka, *Chem. Commun.* **2007**, 2938.
163 S. Saito, A. Osuka, *Chem.—Eur. J.* **2006**, *12*, 9095.
164 P. J. Chmielewski, *Angew. Chem., Int. Ed.* **2010**, *49*, 1359.
165 a) Z.-L. Xue, Z. Shen, J. Mack, D. Kuzuhara, H. Yamada, T. Okujima, N. Ono, X.-Z. You, N. Kobayashi, *J. Am. Chem. Soc.* **2008**, *130*, 16478. b) D. Kuzuhara, H. Yamada, Z. Xue, T. Okujima, S. Mori, Z. Shen, H. Uno, *Chem. Commun.* **2011**, *47*, 722. c) Z. L. Xue, J. Mack, H. Lu, L. Zhang, X. Z. You, D. Kuzuhara, M. Stillman, H. Yamada, S. Yamauchi, N. Kobayashi, Z. Shen, *Chem.—Eur. J.* **2011**, *17*, 4396. d) K. S. Anju, S. Ramakrishnan, A. Srinivasan, *Org. Lett.* **2011**, *13*, 2498.

Award recipient

Atsuhiro Osuka received a Ph.D. from Kyoto University in 1982. In 1979, he started his academic carrier at Ehime University as an Assistant Professor. In 1984, he moved to Kyoto University, where he became a Professor in 1996. He received the Japanese Photochemistry Award in 1999 and the Chemical Society of Japan Award in 2009. His research interests cover many aspects of synthetic approaches toward novel porphyrin-related compounds with intriguing structures, properties, and functions. Representative molecules explored in his laboratory include artificial photosynthetic reaction center models, *meso–meso*-linked porphyrin arrays, porphyrin tapes, *meso*-aryl expanded porphyrins, subporphyrins, and Möbius aromatic and antiaromatic molecules.

Eiji Tsurumaki was born in 1984 in Niigata, Japan. He received his B.Sc. (2007) and M.Sc. (2009) degrees from Kyoto University. He is currently a Ph.D. student with Prof. A. Osuka at the same university, focusing on subporphyrin chemistry. During winter 2010, he worked with Prof. Christopher A. Reed's group at the University of California, Riverside. He was selected as a Research Fellow of the Japan Society for the Promotion of Science for young scientists in 2009.

Takayuki Tanaka was born in 1984 in Osaka, Japan. He received his B.Sc. (2007) and M.Sc. (2009) degrees from Kyoto University. He is currently a Ph.D. student with Prof. Osuka at the same university. During autumn 2010, as a visiting fellow, he worked with Prof. Jeremy K. M. Sanders's group at the University of Cambridge. He was selected as a Research Fellow of the Japan Society for the Promotion of Science for young scientists in 2009.